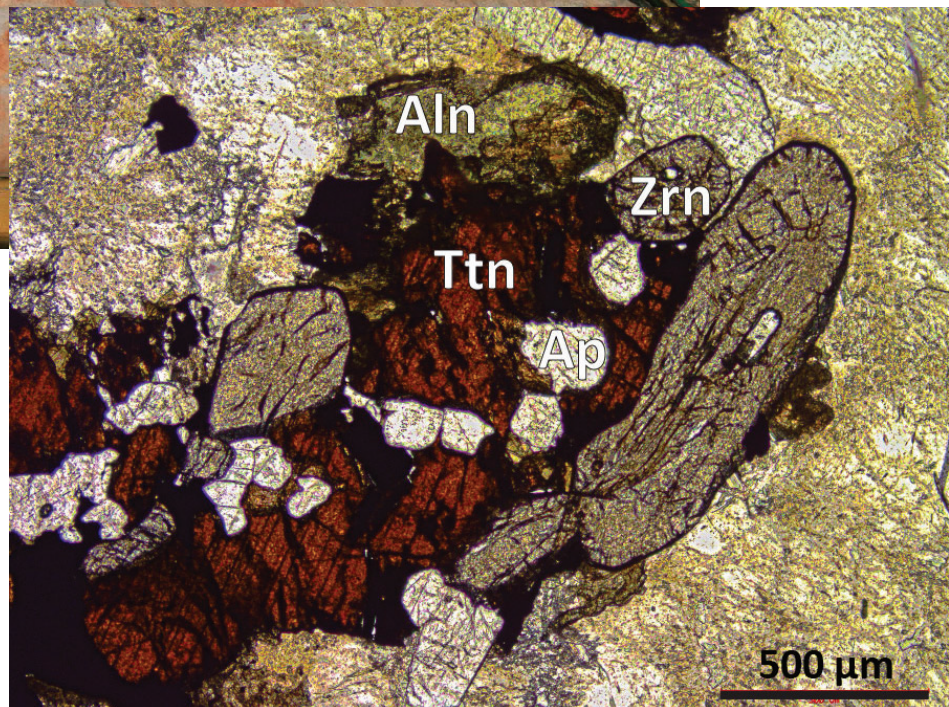
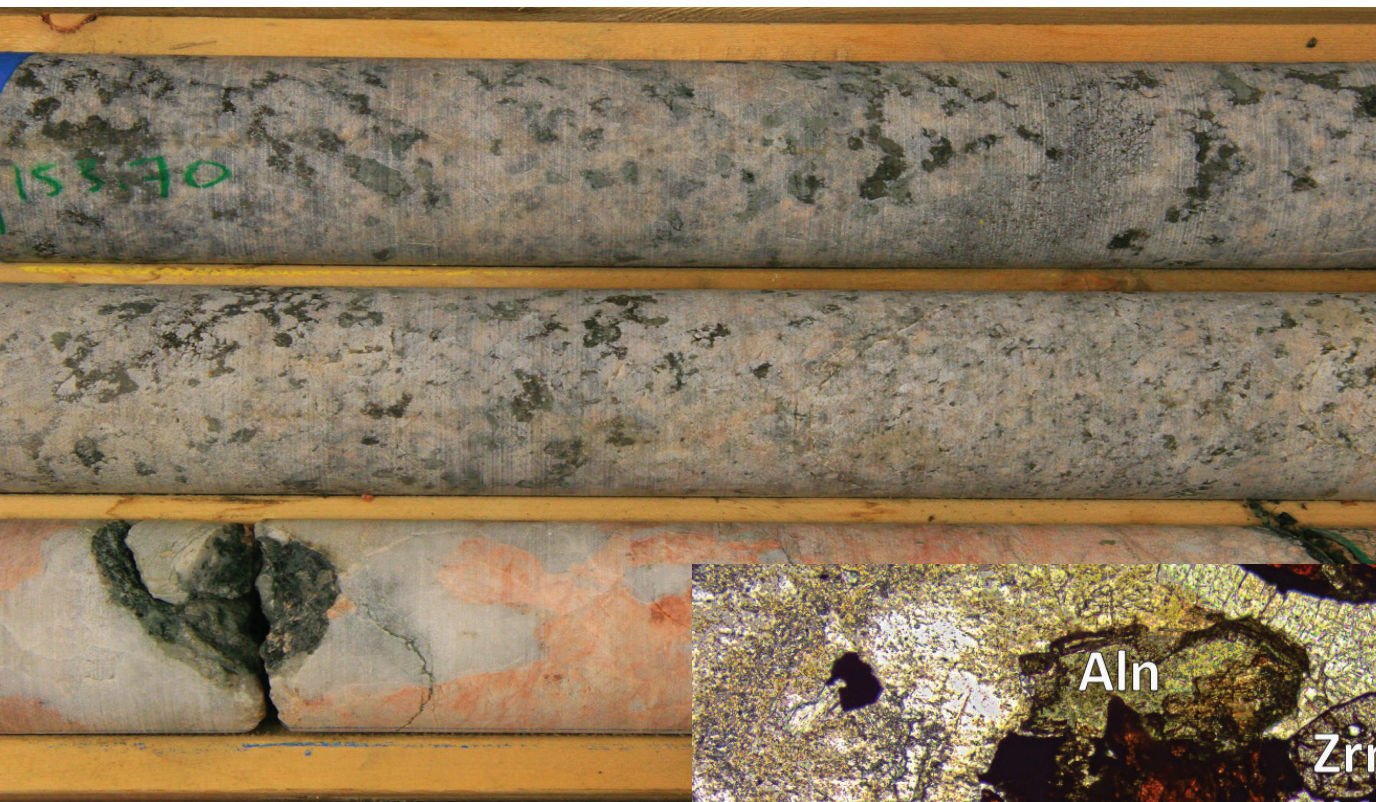


Open File OF2023-2

Age and petrology of zirconium- and light rare-earth element-enriched quartz monzonite in drillcore from the Huzyk Creek property, sub-Phanerozoic Kiseeynew domain, central Manitoba (NTS 63J6)





Open File OF2023-2

**Age and petrology of zirconium- and light rare-earth
element-enriched quartz monzonite in drillcore from the
Huzyk Creek property, sub-Phanerozoic Kisseynew domain,
central Manitoba (NTS 63J6)**

**by C.G. Couëslan
Manitoba Geological Survey
Winnipeg, 2023**

Every possible effort is made to ensure the accuracy of the information contained in this report, but Manitoba Economic Development, Investment and Trade does not assume any liability for errors that may occur. Source references are included in the report and users should verify critical information.

Any third party digital data and software accompanying this publication are supplied on the understanding that they are for the sole use of the licensee, and will not be redistributed in any form, in whole or in part. Any references to proprietary software in the documentation and/or any use of proprietary data formats in this release do not constitute endorsement by Manitoba Economic Development, Investment and Trade of any manufacturer's product.

When using information from this publication in other publications or presentations, due acknowledgment should be given to the Manitoba Geological Survey. The following reference format is recommended:

Couëslan C.G. 2023: Age and petrology of zirconium- and light rare-earth element-enriched quartz monzonite in drillcore from the Huzyk Creek property, sub-Phanerozoic Kisseynew domain, central Manitoba (NTS 63J6); Manitoba Economic Development, Investment and Trade, Manitoba Geological Survey, Open File OF2023-2, 28 p., 1 appendix.

NTS grid: 63J6

Published by:

Manitoba Economic Development, Investment and Trade
Manitoba Geological Survey
360–1395 Ellice Avenue
Winnipeg, Manitoba
R3G 3P2 Canada

Telephone: 1-800-223-5215 (General Enquiry)

204-945-6569 (Publication Sales)

Fax: 204-945-8427

Email: minesinfo@gov.mb.ca

Website: manitoba.ca/minerals

ISBN: 978-0-7711-1646-9

This publication is available to download free of charge at manitoba.ca/minerals.

This publication is available in alternate formats upon request.

Front cover photos:

Top left: Diamond-drill core of the Huzyk Creek quartz monzonite (top two rows) and pegmatitic granite (bottom row).

Bottom right: Photomicrograph in plane-polarized light of zircon, titanite, apatite and allanite in quartz monzonite sample 108-20-HZ03. Abbreviations: Aln, allanite; Ap, apatite; Ttn, titanite; Zrn, zircon.

Abstract

Examination of drillcore from the Huzyk Creek property has revealed the presence of hornblende monzonitic and metasomatic rocks crosscutting metamorphosed mafic rocks and wackes of the sub-Phanerozoic Kiseynew domain. The 'monzonite' ranges in composition from monzonite to quartz syenite to granite, and is massive to weakly foliated. Mafic minerals are dominated by clinopyroxene and secondary amphibole, or hornblende, biotite, and secondary amphiboles. Evidence for metasomatism of the monzonite is present as microveinlets of carbonate±biotite, and the presence of both perthitic and antiperthitic feldspar. Likely related metasomatic rocks in the drillcore are present as discordant calcsilicate rock, bleached zones in tonalite, and sulphide- and garnet-rich calcsilicate veins. The monzonite and related metasomatic rocks are generally enriched

in Ba, Sr, light rare-earth elements (LREE), and in the case of the monzonite, Zr. Magmatic zircon U-Pb geochronology yielded an interpreted age of 1800.5 ± 2.4 Ma for the monzonite. Whole-rock Sm-Nd isotope geochemistry yielded a juvenile initial ϵ_{Nd} value of +1.7 at 1.80 Ga. The monzonite at Huzyk Creek is petrographically, geochemically and geochronologically similar to high-K calcalkaline to shoshonitic syenitic complexes in the Trans-Hudson orogen of Manitoba. Several of these syenitic complexes have been explored for U, Th, REE and P, and two of the complexes contain carbonatite dikes. No carbonatite was identified in the drillcore at Huzyk Creek; however, it is possible that the microveinlets of carbonate±biotite could be related to carbonatite magmatism. Isotopic and mineral geochemical studies of the carbonatite veinlets may be warranted.

Résumé

L'examen des carottes prélevées dans la propriété du ruisseau Huzyk a révélé la présence de roches métasomatiques et monzonitiques à hornblende qui traversent les roches mafiques et les wackes métamorphisés du domaine de Kiseynew subphanérozoïque. Les roches « monzonitiques » varient en composition (monzonite, syénite quartzique, granit, etc.) et en structure, de massive à faiblement foliée. Les minéraux mafiques sont dominés soit par les clinopyroxènes et les amphiboles secondaires soit par les amphiboles hornblende, biotites et secondaires. La métasomatose de la monzonite est confirmée par la présence de micro-filonnets de carbonate±biotite, ainsi que par la présence de feldspath perthitique et antiperthitique. Des roches métasomiques probablement associées sont présentes dans les carottes sous forme de roches calco-silicatées discordantes, de zones décolorées en tonalite et de veines calco-silicatées riches en soufre et en grenats. La monzonite et les roches métasomiques connexes sont généralement enrichies de baryum, de

strontium, d'éléments des terres rares (ETR) légères et, dans le cas de la monzonite, de zirconium. La géochronologie U-Pb sur zircons en domaine magmatique a donné pour la monzonite un âge interprété de $1800,5 \pm 2,4$ Ma. La méthode isotopique Sm-Nd sur roche totale a donné une valeur ϵ_{Nd} initiale juvénile de +1,7 à 1,80 Ga. La monzonite présente au ruisseau Huzyk est sur les plans pétrographique, géochimique et géochronologique similaire aux complexes syénitiques calco-alcalins à shoshonitiques à forte teneur en potassium de l'orogène trans-hudsonien du Manitoba. Plusieurs de ces complexes syénitiques ont été explorés à la recherche d'uranium, de thorium, d'ETR et de phosphore, et deux d'entre eux contiennent des filons carbonatitiques. Aucune carbonatite n'a été relevée dans les carottes prélevées au ruisseau Huzyk; il est toutefois possible que les micro-filonnets de carbonate±biotite soient liés au magmatisme carbonatitique. Des études géochimiques isotopiques et minérales des filonnets de carbonatite pourraient s'avérer nécessaires.

TABLE OF CONTENTS

	Page
Abstract / Résumé	iii
Introduction.....	1
Regional geology	1
Sub-Phanerozoic Kisseynew domain.....	1
Geology of the Huzyk Creek drillcore	1
Granitoid rocks and possible metasomatic phases	2
Foliated tonalite	3
Foliated quartz monzodiorite	4
Foliated biotite granite	4
Quartz monzonite.....	4
Aplitic granite	5
Massive biotite granite	5
Pegmatitic granite	7
Calcsilicate	7
Bleached tonalite.....	9
Lithogeochemistry.....	9
Sampling and analytical methods	9
Granitoid rocks.....	10
Calcsilicate and bleached tonalite.....	12
Radiogenic isotope analyses.....	13
Zircon U-Pb geochronology.....	13
Whole-rock Sm-Nd isotope geochemistry	16
Discussion.....	16
Possible metasomatic phases	21
Economic considerations.....	25
Acknowledgments.....	26
References.....	26

TABLES

Table 1: Summary of lithogeochemical results for representative samples of granitoids, sulphide- and titanite-rich calcsilicate, and bleached tonalite from the Huzyk Creek property	11
Table 2: U-Pb ID-TIMS analytical data for zircon fractions from quartz monzonite sample 108-20-HZ03	17
Table 3: Summary of Sm-Nd whole-rock isotopic data for quartz monzonite sample 108-20-HZ03.....	18

FIGURES

Figure 1: Tectonic-elements map of the Manitoba–Saskatchewan segment of the Trans-Hudson orogen	2
Figure 2: Schematic log of drillcore HZ-19-1 from the Huzyk Creek property	3
Figure 3: Drillcore images of country rock from drillhole HZ-19-1	4
Figure 4: Huzyk Creek granitoid compositions plotted on the quartz-alkali feldspar-plagioclase diagram	5
Figure 5: Drillcore images from drillhole HZ-19-1.....	5
Figure 6: Drillcore and thin section images of the quartz monzonite	6
Figure 7: Photomicrographs in cross-polarized light from the quartz monzonite	7
Figure 8: Drillcore and thin section images from drillhole HZ-19-1.....	8

Figure 9: Drillcore and thin section images of sulphide- and titanite-rich calcsilicate	9
Figure 10: Drillcore and thin section images of sulphide-rich calcsilicate	10
Figure 11: Drillcore and thin section images of the bleached tonalite	11
Figure 12: The composition of Huzyk Creek granitoids plotted on the alumina saturation index diagram of Maniar and Piccoli (1989)	13
Figure 13: Chondrite-normalized rare-earth element profiles of Huzyk Creek granitoids	14
Figure 14: Primitive mantle-normalized multi-element profiles of granitoid rocks from the Huzyk Creek drillcore.....	15
Figure 15: Geochemical diagrams for the sulphide- and titanite-enriched calcsilicate and bleached tonalite	16
Figure 16: Zircon separates, fractions, and ID-TIMS results for sample 108-20-HZ03.....	18
Figure 17: K_2O-SiO_2 diagram of Peccerillo and Taylor (1976) showing the composition of Huzyk Creek granitoids.....	19
Figure 18: Chondrite-normalized REE profiles and primitive mantle-normalized multi-element profiles of the foliated granitoids compared to the quartz monzonite.....	20
Figure 19: Chondrite-normalized REE profiles and primitive mantle-normalized multi-element profiles of the massive granitoids compared to the quartz monzonite.....	20
Figure 20: Discrimination diagrams showing the compositions of Huzyk Creek granitoids	21
Figure 21: Chondrite-normalized REE profiles and primitive mantle-normalized multi-element profiles of representative A-type granite suites compared to the Huzyk Creek quartz monzonite.....	22
Figure 22: Discrimination diagrams showing the compositions of high-K to shoshonitic suites from the Trans-Hudson orogen, the Paint Lake syenite from the Thompson nickel belt, and the Huzyk Creek quartz monzonite	23
Figure 23: Chondrite-normalized REE profiles and primitive mantle-normalized multi-element profiles of the Paint Lake syenite compared to the Huzyk Creek quartz monzonite	23
Figure 24: Chondrite-normalized REE profiles and primitive mantle-normalized multi-element profiles of high-K to shoshonitic suites from the Trans-Hudson orogen compared to the Huzyk Creek quartz monzonite	24
Figure 25: Normalized trace-element profiles of the bleached tonalite and calcsilicate compared to the unaltered tonalite, mafic gneiss suite, and quartz monzonite	25

DIGITAL DATA

Appendix: Supplementary drillcore log for HZ-19-1 with accompanying photos.....	OF2023-2.zip
---	--------------

Introduction

A project was initiated in 2019 to investigate the origins of vanadium-enriched graphite mineralization in drillcore from the Huzyk Creek property (Beaumont-Smith, 2018; Couëslan, 2019, 2020a, 2022; Vanadian Energy Corporation, 2019). During this investigation, a sample of hornblende granite from drillcore HZ-19-1 was found to contain elevated concentrations of Ba, Sr, Zr, and light rare-earth elements (LREE; Couëslan, 2020a). In addition, sparse calcsilicate rocks that appeared to crosscut regional structural fabrics were tentatively interpreted as metasomatic in origin. Similar rocks are associated with several high-K to shoshonitic syenitic complexes in the Trans-Hudson orogen of Manitoba (Couëslan, 2005; Chakhmouradian et al., 2008; Martins et al., 2011, 2012a; Hnatiuk et al., 2022; Martins and Couëslan, 2022); however, the high Zr and rare-earth elements (REE) values of the granite are also suggestive of A-type affinity granitoids. A new study was initiated in 2020 to determine the extent and nature of the enriched granite and the possible origins of the crosscutting calcsilicate rocks (Couëslan, 2020b).

During the 2019 investigation, the drillcore was logged by attempting to discern the original protolith of the high-grade gneisses through the metamorphic and magmatic overprint (Couëslan, 2019). In 2020, a portion of drillcore HZ-19-1 was revisited looking specifically at intrusive phases and possible metasomatic overprint. This report will concentrate on the magmatic and possible metasomatic phases present in the drillcore. For a more detailed description of the host rocks, the reader is referred to Couëslan (2020a, 2022).

Regional geology

Although the Huzyk Creek property overlies the boundary between the Thompson nickel belt and the Kiseynew domain, the stratigraphy, lithogeochemistry, and Sm-Nd isotope geochemistry indicate drillholes HZ-19-1 and HZ-19-2 intersect rocks of the sub-Phanerozoic Kiseynew domain (Figure 1; Couëslan, 2020a). The Kiseynew domain is situated in the core of the juvenile Reindeer zone of the Paleoproterozoic Trans-Hudson orogen (THO). It is underlain by dominantly Burntwood group rocks, with subordinate calcalkaline plutons and sheets of anatectic granitoids. The Burntwood group forms a monotonous sequence of graphite-bearing metagreywacke-mudstone, which was metamorphosed to garnet-biotite gneiss and migmatite throughout much of the Kiseynew domain during the terminal collision of the THO. The metagreywacke-mudstone is interpreted as turbidite deposits shed from the surrounding juvenile accretionary-arc complexes of the Flin Flon and Lynn Lake domains (Ansdell et al., 1995; Zwanzig and Bailes, 2010). Coeval fluvial-alluvial deposits on the margins of these volcano-plutonic domains consist of the Missi and Sickle groups, respectively (Stauffer, 1990; Zwanzig and Bailes, 2010; Murphy and Zwanzig, 2021). The Kiseynew paleobasin is generally interpreted as a back-arc basin; however, an inter-arc or fore-arc basin environment is also possible (Ansdell et al., 1995; Zwanzig, 1997; Corrigan et al., 2009; Zwanzig and Bailes, 2010; Murphy and Zwanzig, 2021).

Several high-K calcalkaline to shoshonitic syenitic complexes occur in the Kiseynew domain and adjacent parts of the THO (Figure 1). These complexes are dominated by silica saturated syenitic to monzonitic rocks with subordinate granitic rocks, and rare carbonatite and lamprophyre dikes (Couëslan, 2005; Chakhmouradian et al., 2008; Martins et al., 2011, 2012a; Hnatiuk et al., 2022; Martins and Couëslan, 2022). The silicate rocks in the shoshonite complexes are generally enriched in K, Ba, Sr, and LREE. Carbonatite dikes and veins of REE mineralization occur at the Eden Lake complex (Couëslan, 2005; Mumin, 2010), and a carbonatite dike was recently identified along with lamprophyre-like dikes at the Brezden Lake complex (Hnatiuk et al., 2022). The shoshonitic complexes are interpreted as late orogenic and range in age from ca. 1829 Ma (Brezden Lake) to ca. 1794 Ma (Burntwood Lake; Martins, unpublished data, 2022).

Sub-Phanerozoic Kiseynew domain

The sub-Phanerozoic Kiseynew domain is the southern extension of the Kiseynew domain below the Phanerozoic cover (Figure 1). Situated between the Superior craton margin and the Flin Flon domain, it was interpreted to consist of migmatitic metasedimentary rocks of the Burntwood group interlayered with felsic metaplutonic veins and sheets (Leclair et al., 1997). However, the discovery of several volcanogenic massive sulphide (VMS) deposits (Watts River, Harmin, Fenton and Talbot) in the domain has brought this interpretation into question (Simard et al., 2010). Recent studies (Simard et al., 2010; Bailes, 2015; Reid, 2018) suggest complex structural interleaving of Flin Flon domain arc rocks, Kiseynew domain Burntwood group rocks, and possibly Thompson nickel belt rocks within the sub-Phanerozoic Kiseynew domain. A similar situation occurs along the north, south and east flanks of the exposed Kiseynew domain, where thrusts and recumbent folding have structurally interleaved rocks of the Kiseynew basin with rocks of adjacent juvenile volcano-plutonic terranes and evolved Archean crust (Zwanzig, 1999; Rayner and Percival, 2007; Zwanzig and Bailes, 2010; Murphy and Zwanzig, 2021).

Geology of the Huzyk Creek drillcore

The core from two drillholes (HZ-19-1 and HZ-19-2) were logged in August of 2019 to investigate vanadium-enriched graphite mineralization on the property. The Huzyk Creek drillcore consists of a hornblende gneiss and calcsilicate package in contact, and locally interleaved, with a wacke-mudstone succession containing the metal-enriched graphite mineralization (Figure 2; Couëslan, 2020a, 2022). The hornblende gneiss and calcsilicate can be interlayered on scales ranging from <1 cm to 2.5 m, with diffuse contacts (Figure 3a). They are interpreted as variably altered mafic rocks, and may be related to Missi-age, successor-arc magmatism (Couëslan, 2020a). For the purpose of this report, the hornblende gneiss and calcsilicate package will be referred to as the 'mafic gneiss suite' in order to avoid confusion with other calcsilicate phases discussed below. The mafic gneiss suite occurs at the top of the Precambrian in both

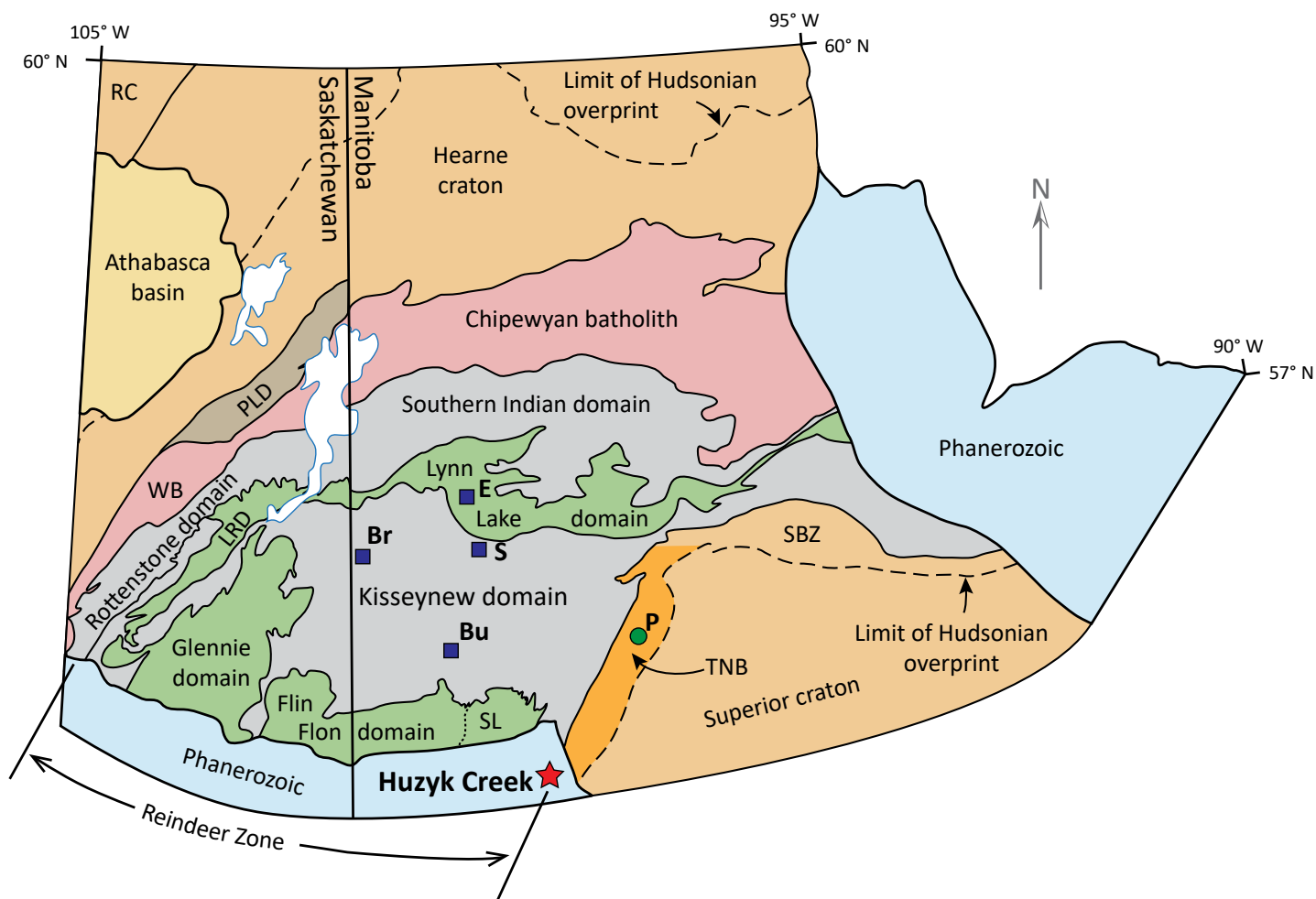


Figure 1: Tectonic-elements map of the Manitoba–Saskatchewan segment of the Trans-Hudson orogen (modified from Lewry et al., 1990; Maxeiner et al., 2021; Manitoba Geological Survey, 2022). The approximate location of Huzyk Creek drillhole HZ-19-1 is indicated with a red star. Blue squares indicate the locations of high-K to shoshonitic syenite complexes in the Trans-Hudson orogen. The green circle indicates the location of the Paint Lake syenite. Abbreviations: Br, Brezden Lake complex; Bu, Burntwood Lake complex; E, Eden Lake complex; LRD, La Ronge domain; P, Paint Lake syenite; PLD, Peter Lake domain; RC, Rae craton; S, Suwannee River complex; SBZ, Superior boundary zone; SL, Snow Lake subdomain; TNB, Thompson nickel belt; WB, Wathaman batholith.

drillholes; however, the stratigraphic younging direction is not known. In drillhole HZ-19-1 the mafic gneiss suite is interleaved with the underlying wacke-mudstone at a scale of 2.6 to 35 m. A preserved contact between the mafic gneiss suite and the wacke is sharp with no significant change in strain across the contact (Figure 3b). This may suggest a contact that is stratigraphic rather than tectonic (faulted or sheared). The wacke-mudstone package consists of migmatitic gneisses that are subdivided according to the dominant mafic mineral other than biotite. They consist of orthopyroxene wacke-mudstone with subordinate garnet wacke-mudstone (Figure 3c) and graphite mudstone (Figure 3d), and rare hornblende wacke-mudstone. The various wacke-mudstone units are interlayered at a scale of <1 cm to several m with the exception of the graphite mudstone, which occurs as a discrete horizon roughly 15 m thick. The wacke-mudstone package appears to be related to the Burntwood group of the Kisseynew domain, and was likely deposited relatively proximal to the Flin Flon arc-collision (Couëslan, 2020a, 2022).

The gneisses outlined above were intruded by several phases of granitoid rocks ranging from tonalite to granite. The intrusions range in size from several cm up to roughly 20 m. Most intrusions have a well-defined foliation except for a coarse-grained, hornblende-bearing quartz monzonite that is massive to weakly foliated, and a medium-grained biotite granite that is massive. Intrusions of aplitic granite and pegmatitic granite vary from strongly foliated to relatively massive and likely consist of several generations.

Granitoid rocks and possible metasomatic phases

Approximately 190 m (from 71.5 to 262.9 m) of drillcore HZ-19-1 was relogged and sampled in July 2020 (Figure 2; Appendix). The focus of this study was to document the quartz monzonite, other granitoid rocks, and possible evidence of related metasomatic overprint in the core. Although definitive examples of metasomatism are rare, two phases of potential interest were recognized in the core: sulphide- and titanite-rich calcsilicate,

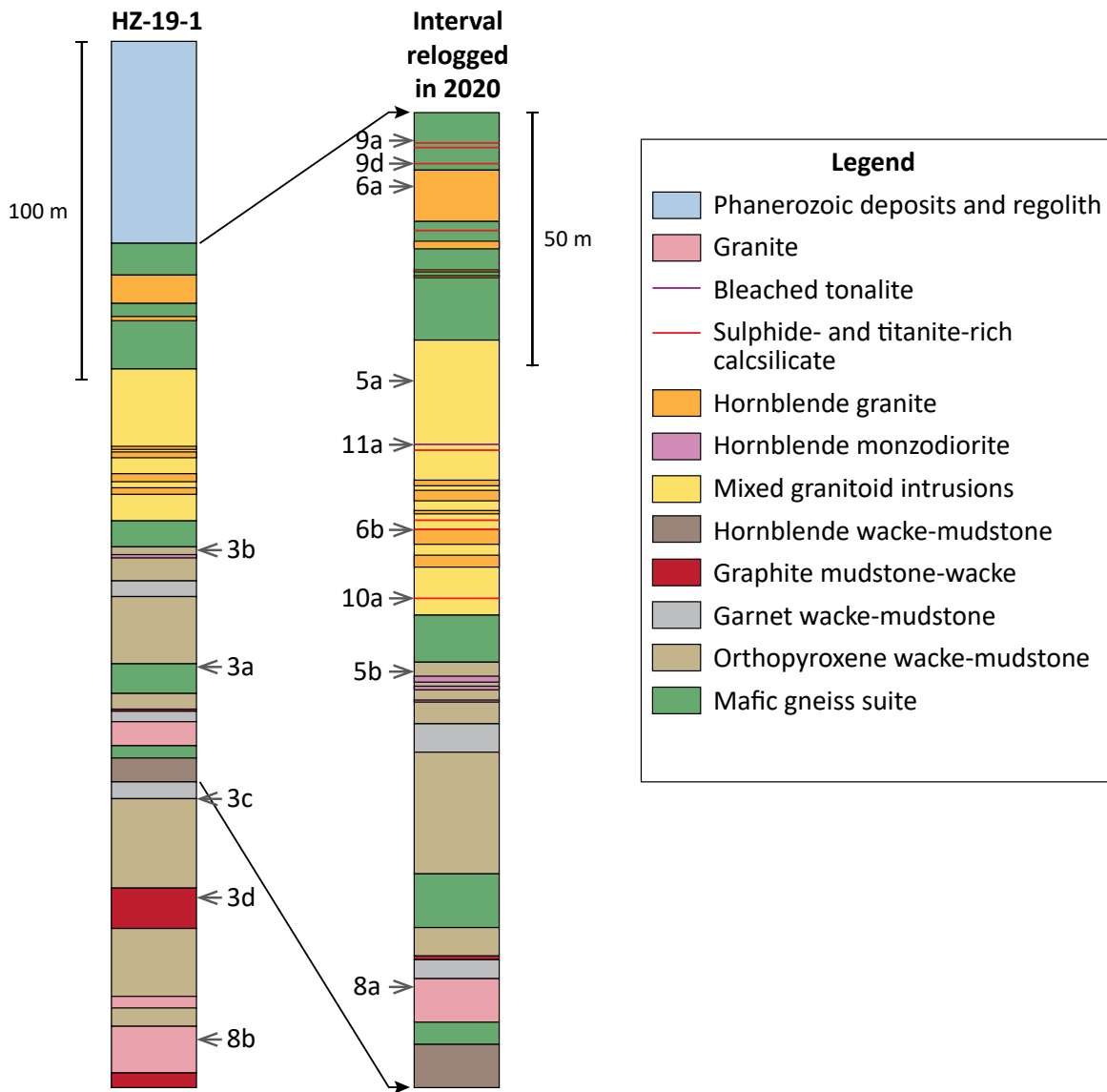


Figure 2: Schematic log of drillcore HZ-19-1 from the Huzyk Creek property, including a more detailed section of the interval that was revisited in 2020. Thicknesses of sulphide- and titanite-rich calcsilicate, and bleached tonalite are not to scale. The stratigraphic positions of core images in Figures 3, 5, 6, and 8–11 are indicated along the inside edge of each column.

and a zone of bleached tonalite. These phases, along with the hornblende quartz monzonite, appear to be restricted to the upper 116 m of the Precambrian (from 71.5 to 187.3 m). Samples of massive biotite granite were collected from outside of the relogged interval at 340 m and 355.5 m. Compositions were determined with point counts of at least 640 points for the quartz monzonite and aplite, and at least 340 points for the other granitoid phases (Figure 4). The granitoid phases are described in order from foliated to relatively non-foliated phases, and from more tonalitic/dioritic compositions to more granitic compositions. Reported thicknesses in this report are intersection lengths, not true thicknesses.

Foliated tonalite

The tonalite occurs as relatively sparse dikes, <6 m wide, throughout the drillcore, but is most abundant in the multicom-

ponent gneiss interval from 116–170 m (Figure 2). It varies from white to pinkish grey and is coarse grained, foliated to strongly foliated, and non-magnetic (Figure 5a). Two of the samples plot as tonalite on the quartz–alkali feldspar–plagioclase diagram, while one sample plots as quartz diorite (Figure 4). Because the three samples are mineralogically and geochemically similar they are described under one unit and will be collectively referred to as tonalite. The mafic mineral content ranges from 17 to 41%. More mafic-rich examples (>25% mafic minerals) typically consist of hornblende-biotite tonalite with a roughly 1:2 ratio of hornblende to biotite. More felsic varieties consist of biotite tonalite and contain only minor amounts of hornblende. Potassium feldspar is typically present in trace amounts, but can be as high as 3% in the biotite tonalite. Antiperthite is present in all varieties of tonalite. Accessory minerals in the tonalite include titanite, Fe-oxide, apatite, and zircon. Secondary chlorite, carbonate, and muscovite can also be present.

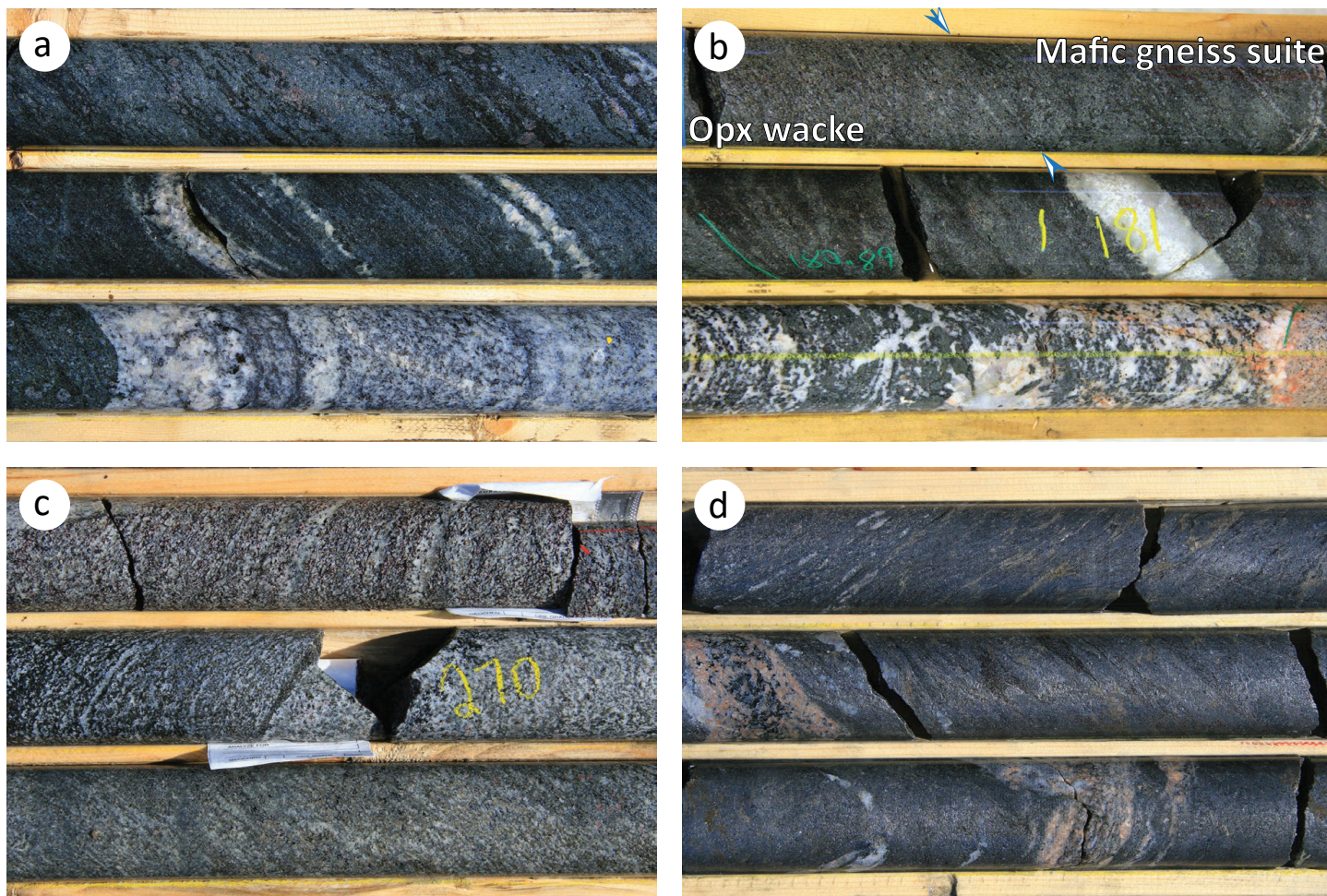


Figure 3: Drillcore images of country rock from drillhole HZ-19-1: **a)** diffusely interlayered calcsilicate and hornblende gneiss (mafic gneiss suite; top two rows), and foliated biotite granite (bottom row; 221.65 m); **b)** contact between orthopyroxene (Opx) wacke and mafic gneiss suite (top row, marked with arrows), mafic gneiss suite (middle row), and foliated quartz monzodiorite (bottom row; 179.4 m); **c)** interbedded garnet wacke (top row) and orthopyroxene wacke (bottom row; 268.5 m); **d)** graphite mudstone (303.2 m).

Foliated quartz monzodiorite

The quartz monzodiorite occurs from 182.0 to 187.3 m as dikes <1.2 m thick. The dikes are pale pink to greenish white, coarse grained and foliated (Figures 3b, 5b). Mafic minerals constitute roughly 20% of the rock and are dominated by amphibole and clinopyroxene along with minor biotite and iron oxide. Two varieties of amphibole are present. The most common variety of amphibole occurs as fine- to medium-grained polycrystalline aggregates and rims enclosing clinopyroxene. Less common are discrete medium to coarse grains of amphibole. Biotite is commonly intergrown with the amphibole aggregates, and occurs as sparse partial rims on the discrete amphibole grains. Biotite also occurs along with carbonate in microveinlets. The mafic minerals define a well developed foliation. Iron oxide commonly has thin rims of titanite. Titanite can also be present along biotite cleavage planes. Other accessory minerals consist of apatite, allanite and Fe-sulphide.

Foliated biotite granite

Small dikes (<2.7 m) of foliated biotite granite occur throughout the drillcore. The granite is light pinkish grey, medium to

coarse grained, foliated and non-magnetic (Figure 3a). Plagioclase is locally antiperthitic. Zones of recrystallized granophyre are common. Mafic minerals make up 5–12% of the granite and are dominated by biotite. Minor muscovite is present; however, at least some of the muscovite appears to be secondary after feldspar. Other secondary minerals include chlorite, carbonate and epidote. Accessory minerals consist of apatite, zircon and opaques.

Quartz monzonite

The quartz monzonite occurs from the top of the Precambrian (71.5 m) to 160.6 m as dikes up to 10 m, but typically <3 m. It is pink to grey, coarse grained, massive to weakly foliated, and non-magnetic (Figure 6a, b). The composition of the unit ranges from quartz syenite to granite to monzonite (Figure 4), which could indicate multiple phases or inhomogeneous distribution of quartz and feldspars. Although there is a compositional range, this unit will be collectively referred to as quartz monzonite. Mafic mineral content is inversely proportional to the quartz content. Mafic minerals are generally dominated by either clinopyroxene and secondary amphibole, or hornblende, biotite

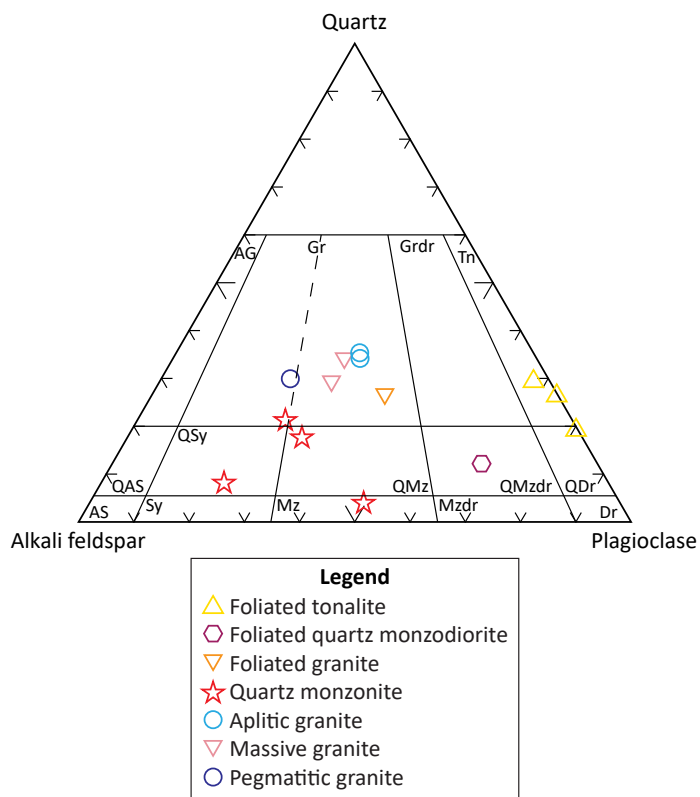


Figure 4: Huzyk Creek granitoid compositions plotted on the quartz-alkali feldspar-plagioclase diagram of Le Maitre (2002). Abbreviations: AG, alkali feldspar granite; AS, alkali feldspar syenite; Dr, diorite; Gr, granite; Grdr, granodiorite; Mz, monzonite; Mzdr, monzodiorite; QAS, quartz alkali feldspar syenite; QDr, quartz diorite; QMz, quartz monzonite; QMzdr, quartz monzodiorite; QSy, quartz syenite; Sy, syenite; Tn, tonalite.

and secondary amphiboles. The secondary amphiboles typically occur as polycrystalline intergrowths that are pseudomorphous after the clinopyroxene (Figure 6c) or primary hornblende (Figure 6d). Amphibole can also occur as rims around clinopyroxene. Primary hornblende is typically partially rimmed or replaced by biotite (Figure 6d). Minor and accessory phases include titanite,

apatite, opaque minerals, zircon, allanite and carbonate (Figure 6e, f). The opaque minerals are typically dominated by either iron sulphide or iron oxide; however, both sulphides and oxides are commonly present.

Evidence for alteration or metasomatism is relatively ubiquitous in samples of the quartz monzonite, with the clinopyroxene-bearing samples appearing the least affected. Carbonate±biotite commonly occurs in microveinlets (Figure 7a), and can be closely associated with allanite, titanite, and opaques (Figure 7b, c). Myrmekite is common and both perthitic and antiperthitic feldspars can be present (Figure 7d). Sparse chlorite occurs as replacement of biotite and both muscovite and epidote can occur as replacement of feldspar.

Aplitic granite

Aplitic granite is common in the drillcore and typically occurs as dikes <50 cm wide, but can be up to 2.75 m. The aplite is pink to grey, and massive to foliated (Figures 6a, 8a). The aplitic granite may consist of several generations, which crosscut all of the units except for the massive biotite granite. Mafic minerals make up less than two percent of the rock and consist dominantly of biotite, muscovite and Fe-sulphide. Other accessory minerals consist of apatite, allanite, monazite and zircon. Chlorite and carbonate occur as secondary minerals.

Massive biotite granite

The massive biotite granite occurs from 339 to 366 m as dikes <16.5 m wide. The granite is red to white, medium to coarse grained, and massive (Figure 8b). Concentric zoning of plagioclase is locally visible in thin sections, and thin discrete sodic rims are common. Biotite makes up 3–5% of the rock. Accessory minerals include zircon, apatite and monazite. Trace amounts of muscovite may be secondary after feldspar. Other secondary minerals include chlorite, carbonate and rutile.

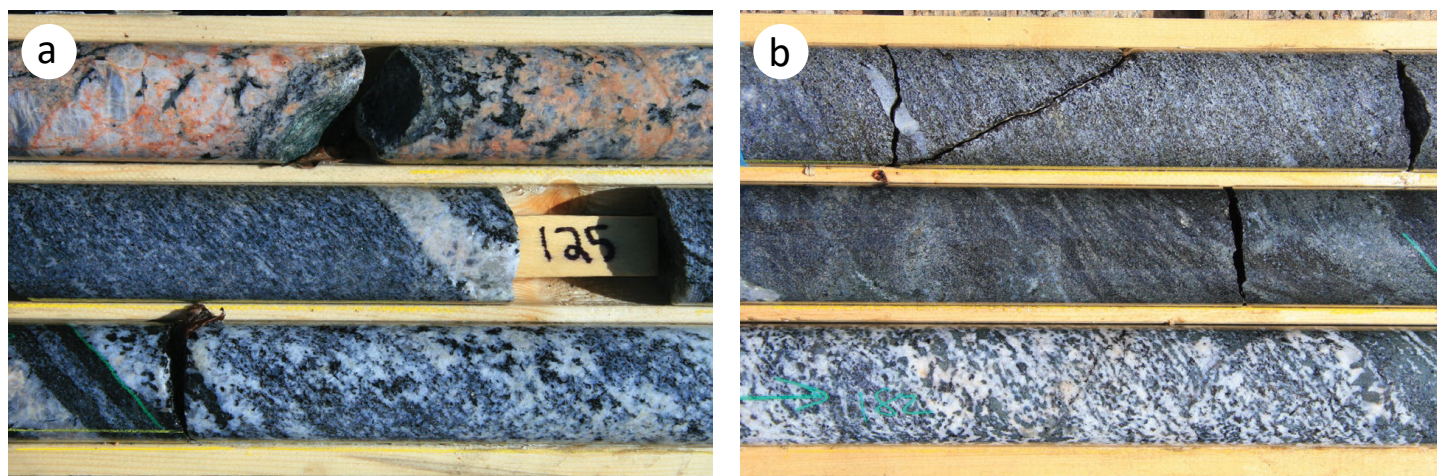


Figure 5: Drillcore images from drillhole HZ-19-1: **a)** foliated pegmatite (top row), mafic-rich foliated tonalite (middle row), and foliated tonalite (bottom row; 123.3 m); **b)** orthopyroxene wacke (top row), mafic gneiss suite (middle row), and foliated monzodiorite (bottom row; 179.1 m).

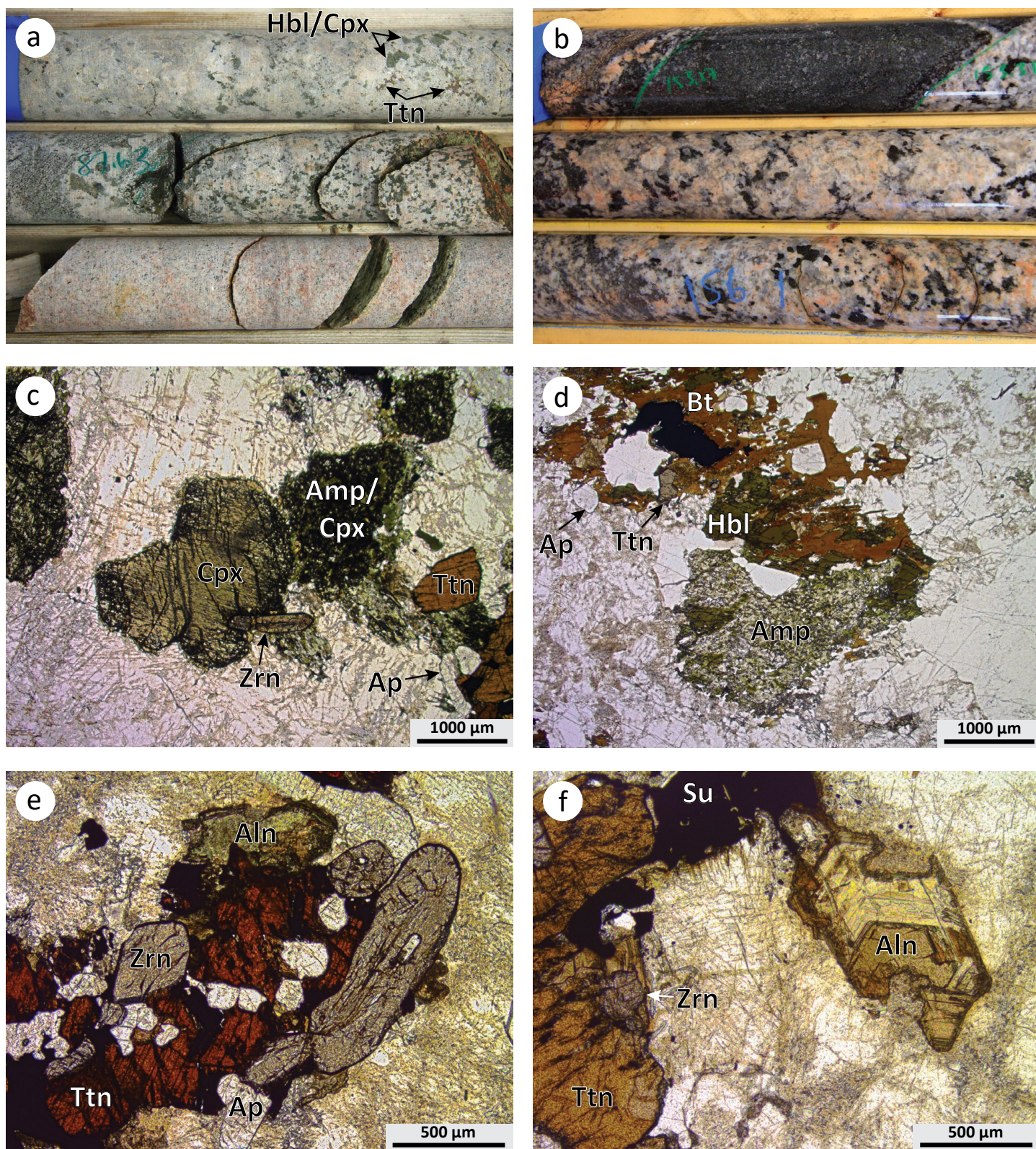


Figure 6: Drillcore and thin section images of the quartz monzonite: **a)** quartz monzonite (top two rows) and aplitic granite (bottom row; 86.0 m); **b)** foliated, titanite-rich calcsilicate (top row) and quartz monzonite (bottom two rows; 153.1 m); **c)** photomicrograph in plane-polarized light (PPL) of clinopyroxene with a thin rim of amphibole adjacent to a polycrystalline aggregate of amphibole with relict clinopyroxene inclusions; **d)** photomicrograph in PPL of primary hornblende partially replaced by biotite and a polycrystalline intergrowth of secondary amphibole; **e)** photomicrograph in PPL of accessory phases in the quartz monzonite including relatively large zircon grains; **f)** photomicrograph in PPL of zoned allanite. Abbreviations: Aln, allanite; Amp, amphibole; Ap, apatite; Bt, biotite; Cpx, clinopyroxene; Hbl, hornblende; Su, Fe-sulphide; Ttn, titanite; Zrn, zircon.

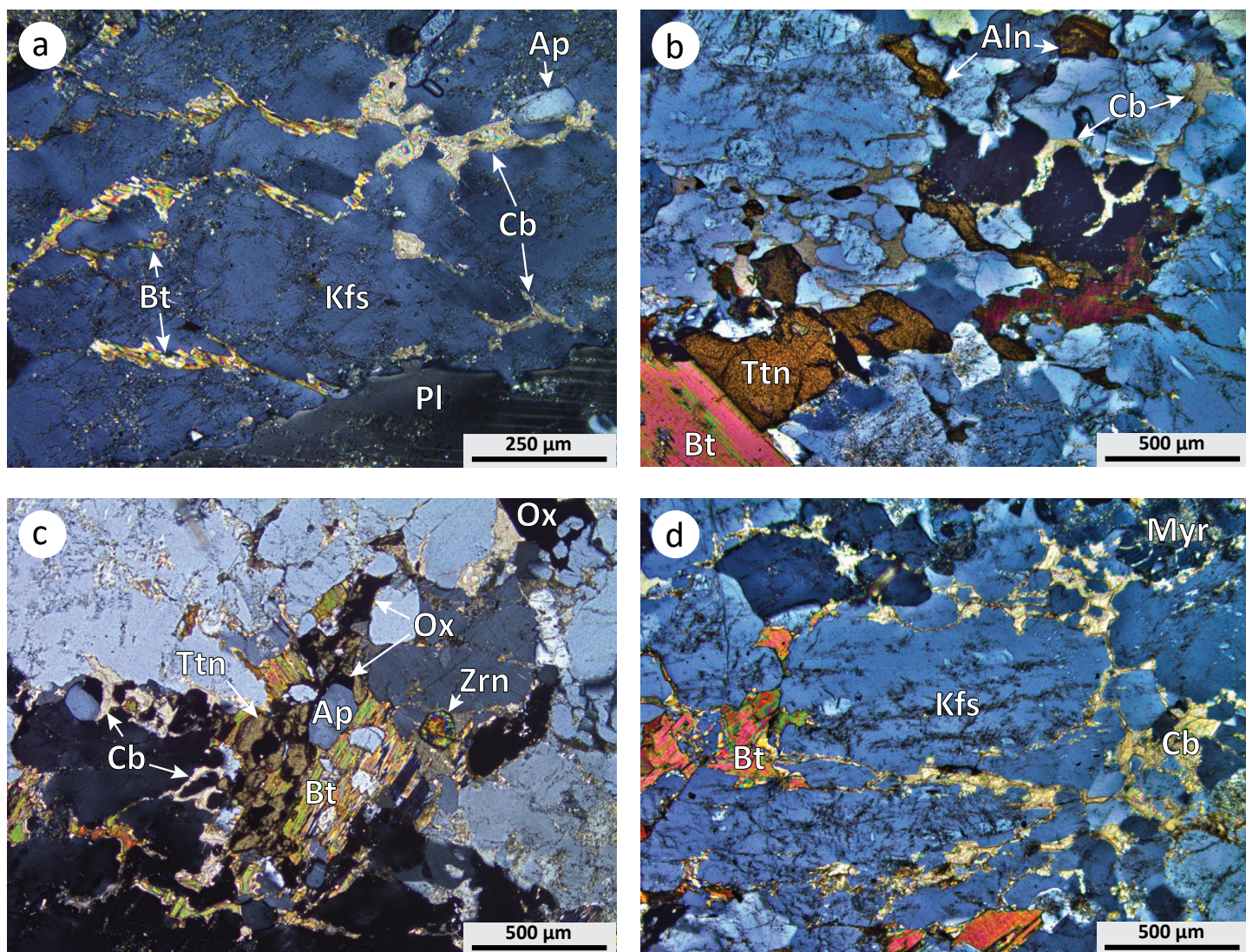


Figure 7: Photomicrographs in cross-polarized light (XPL) from the quartz monzonite: **a)** microveinlets of carbonate and biotite crosscutting perthitic K-feldspar; **b)** titanite and allanite spatially associated with carbonate microveinlets; **c)** titanite and iron oxide spatially associated with carbonate and biotite microveinlets; **d)** carbonate and biotite microveinlets crosscutting perthitic K-feldspar and myrmekite. Abbreviations: Aln, allanite; Ap, apatite; Bt, biotite; Cb, carbonate; Kfs, K-feldspar; Myr, myrmekite; Ox, Fe-oxide; Pl, plagioclase; Ttn, titanite; Zrn, zircon.

Pegmatitic granite

Pegmatitic granite is abundant in the drillcore and forms intersections ranging from centimetres up to 10 m in width. The intrusions range from relatively undeformed to strongly foliated, and they crosscut all units in the drillcore including the massive biotite granite. This suggests that several generations of pegmatite are present. The pegmatitic granite ranges from pink to light grey, and typically contains <5% biotite (Figures 5a, 8a). Accessory minerals include monazite, zircon, allanite and apatite (Figure 8c, d). Secondary minerals include carbonate, chlorite and rutile.

Calcsilicate

Calcsilicate is common from the top of the Precambrian to 254.5 m, where it is diffusely interlayered with hornblende gneiss as part of the mafic gneiss suite, and is interpreted to represent carbonate and/or epidote alteration within mafic igneous

rocks (Couëslan, 2020a). The calcsilicate is plagioclase-rich with 30–40% clinopyroxene and contains trace amounts of carbonate, magnetite, pyrrhotite, titanite and local garnet (Figure 3a). Several examples of anomalously sulphide-rich and titanite-rich calcsilicate were identified in the drillcore. Locally the anomalous calcsilicate appears to overprint the fabric of the country rock; however, it also occurs as xenoliths with a well developed fabric hosted within the quartz monzonite. There are also rare examples of discordant vein-like calcsilicate. The wide textural and mineralogical variability likely indicates multiple ages and origins for the sulphide- and titanite-rich calcsilicate. Examples of each of these varieties were collected and are described separately.

The semiconcordant calcsilicate appears to roughly parallel the fabric of the enclosing hornblende gneiss; however, the margin appears diffuse (Figure 9a). A thin section of semiconcordant calcsilicate reveals a zoned vein-like structure.

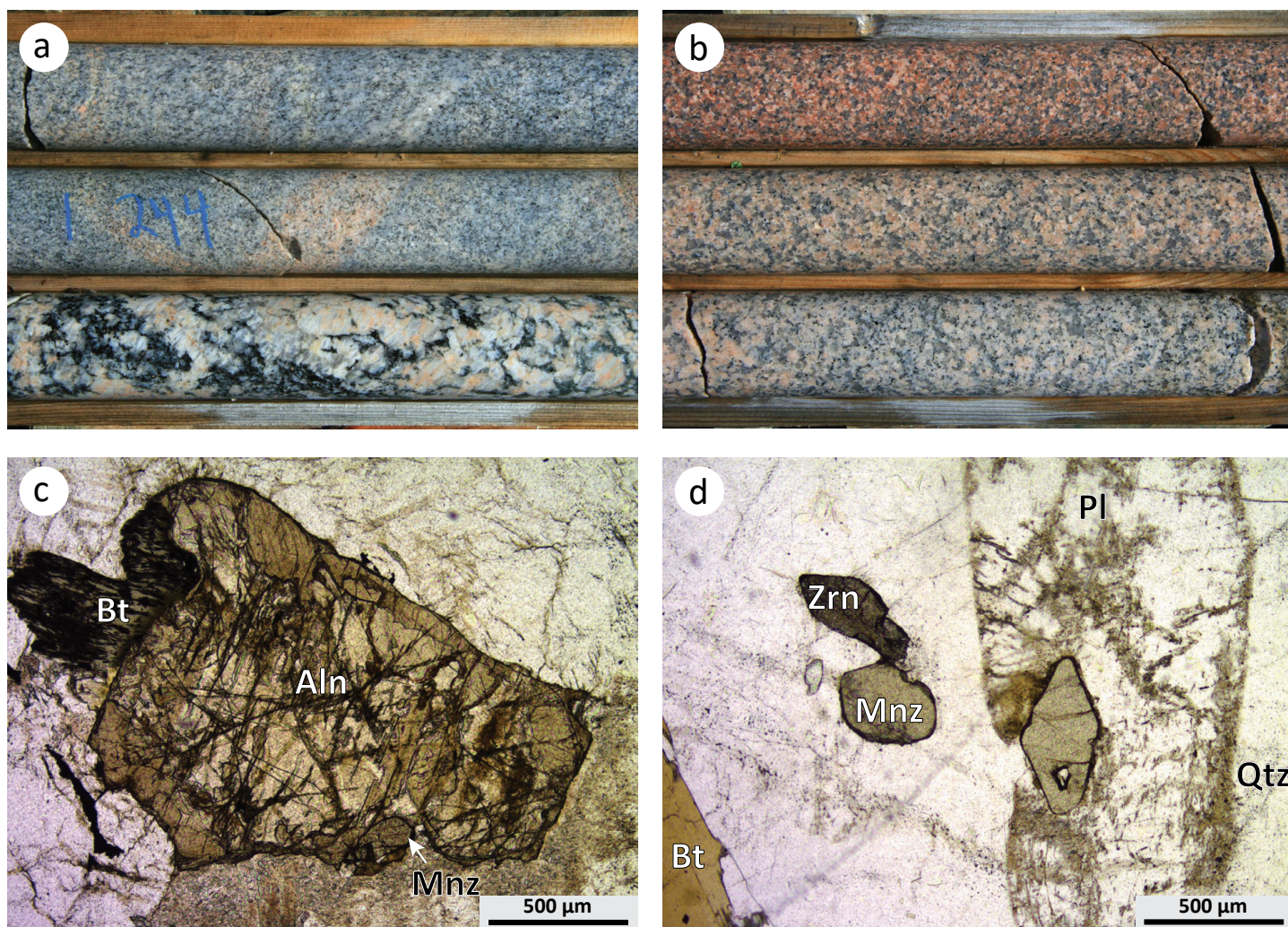


Figure 8: Drillcore and thin section images from drillhole HZ-19-1: **a)** aplitic granite (top two rows) and foliated pegmatite (bottom row; 242.45 m); **b)** massive biotite granite (354.2 m); **c)** photomicrograph in PPL of zoned allanite from pegmatitic granite; **d)** photomicrograph in PPL of zircon and monazite from pegmatitic granite. Abbreviations: Aln, allanite; Bt, biotite; Mnz, monazite; Pl, plagioclase; Qtz, quartz; Zrn, zircon.

The core is plagioclase-rich with 10–20% titanite and 10–20% apatite (Figure 9b). Amphibole (7–10%) occurs as polycrystalline aggregates that pseudomorphously replace clinopyroxene (5–7%). Minor epidote, Fe-sulphide and scapolite are present, and allanite occurs as an accessory phase. The core of the vein is mantled by a plagioclase- and amphibole-rich selvage, which also contains partially replaced clinopyroxene. Minor amounts of titanite, apatite, epidote and Fe-sulphide are present along with sparse carbonate, allanite and scapolite. The foliation of the host rock is preserved within the selvage while the core is not foliated.

The foliated, titanite-rich calcsilicate occurs as a band within the quartz monzonite (Figure 6b). Dikelets of the monzonite intrude the calcsilicate suggesting it likely represents a xenolith of country rock. A thin section of the foliated calcsilicate reveals that it consists of plagioclase-rich and clinopyroxene- and epidote-rich domains. Plagioclase-rich domains contain lesser clinopyroxene and amphibole. Clinopyroxene grains are partially to completely replaced by the amphibole. Minor titanite is present along with Fe-oxide, carbonate and quartz as accessory phases.

Clinopyroxene- and epidote-rich domains also contain amphibole and scapolite, minor titanite, quartz and carbonate (Figure 9c). Apatite, Fe-sulphide, allanite and tremolite occur as accessory phases.

The discordant calcsilicate occurs as a crosscutting vein-like structure in the hornblende gneiss (Figure 9d). It is not foliated and is plagioclase-rich with <10% clinopyroxene that has been variably replaced by amphibole. Minor titanite, apatite, Fe-sulphide and quartz are present. Allanite, epidote and carbonate are present as accessory phases.

The sulphide-rich calcsilicate occurs as a 10 cm thick, zoned vein-like structure (Figure 10a). It is not foliated and has a core consisting largely of pyrrhotite and locally zoned, yellow to brown garnet (Figure 10b). Minor apatite and allanite are present along with a mineral tentatively identified as either zoisite or clinozoisite (Figure 10c). Quartz, carbonate, chalcophyrite, and deep green clinopyroxene occur as accessory minerals. The sulphide-rich core is mantled by a 2–3 cm thick selvage of deep green clinopyroxene with minor epidote and pyrrhotite (Figure 10d). The

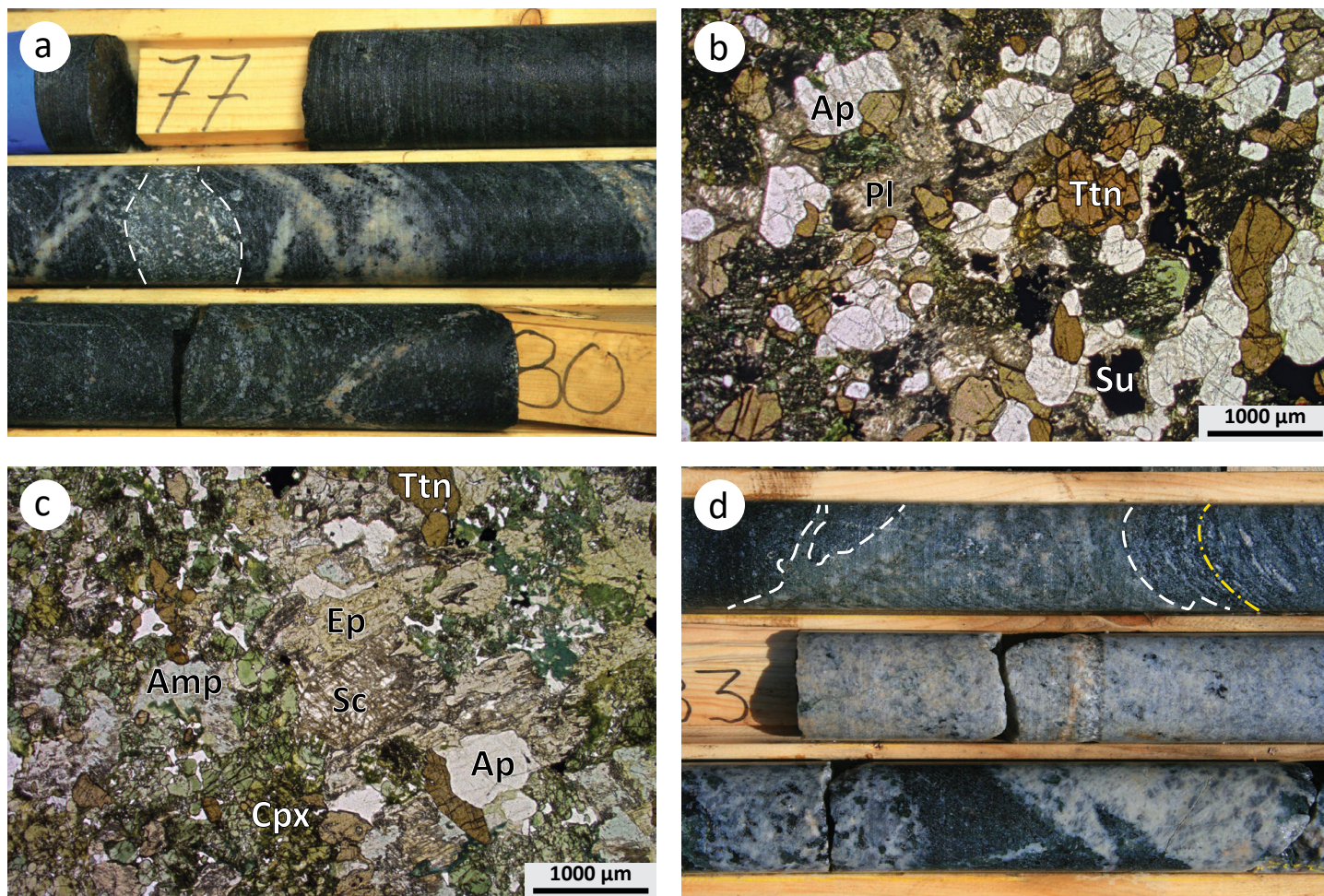


Figure 9: Drillcore and thin section images of sulphide- and titanite-rich calcsilicate: **a)** semiconcordant calcsilicate (middle row, white dashed outline) hosted in mafic gneiss suite rocks (76.95 m); **b)** photomicrograph in PPL of the plagioclase-, titanite- and apatite-rich core of the semiconcordant calcsilicate; **c)** photomicrograph in PPL of a clinopyroxene- and epidote-rich domain in the foliated, titanite-rich calcsilicate; **d)** discordant calcsilicate (top row, white dashed outline) crosscutting the fabric of the mafic gneiss suite rocks (yellow dotted-dashed line), and quartz monzonite intruded into the mafic gneiss suite (bottom two rows; 81.55 m). Abbreviations: Amp, amphibole; Ap, apatite; Cpx, clinopyroxene; Ep, epidote; Pl, plagioclase; Sc, scapolite; Su, Fe-sulphide; Ttn, titanite.

selvage also contains accessory amounts of titanite, apatite and allanite.

Bleached tonalite

A 40 cm thick zone of tonalite with a bleached appearance occurs within the multicomponent gneiss interval (Figure 2). It is light grey, non-foliated, and moderately magnetic with sharp contacts that crosscut fabrics and structures (including xenoliths) in the host tonalite (Figure 11a). The rock consists dominantly of quartz and calcic plagioclase with 10–12% pale green amphibole and clinopyroxene. The plagioclase occurs as a recrystallized, fine-grained felted groundmass that appears to be pseudomorphous after the phaneritic plagioclase of the tonalite (Figure 11b). The quartz appears to be texturally preserved from the tonalitic protolith. Carbonate, titanite and Fe-sulphide occur in minor amounts, and allanite, apatite, garnet and zircon are present as accessory phases. The garnet occurs as relict fragments enclosed by carbonate (Figure 11c). The garnet-carbonate intergrowth is commonly mantled by a rim of clinopyroxene.

Lithogeochemistry

Samples of each of the described units were collected for lithogeochemistry. The results are provided in Couëslan (2020c) and representative analyses are summarized in Table 1.

Sampling and analytical methods

At least one representative sample was collected for each of the described units for geochemical analysis. Approximately 30 cm long samples of representative material were selected from the drillcore. The core was sawn length-wise with one half of the core returned to the core box and the other half being retained for geochemical analysis, thin section, and archive. Samples were crushed to <5 mm at the Manitoba Geological Survey Midland Sample and Core Library using a steel jaw-crusher. Pulps were produced in a steel swing mill and were homogenized by rolling and then splitting to approximately 55 g of analytical material. Two internal standards and one blind duplicate were inserted along with the 20 samples submitted for analysis.

Samples were analyzed at Activation Laboratories Ltd. (Ancaster, Ontario) using the '4Litho' analytical packages, which

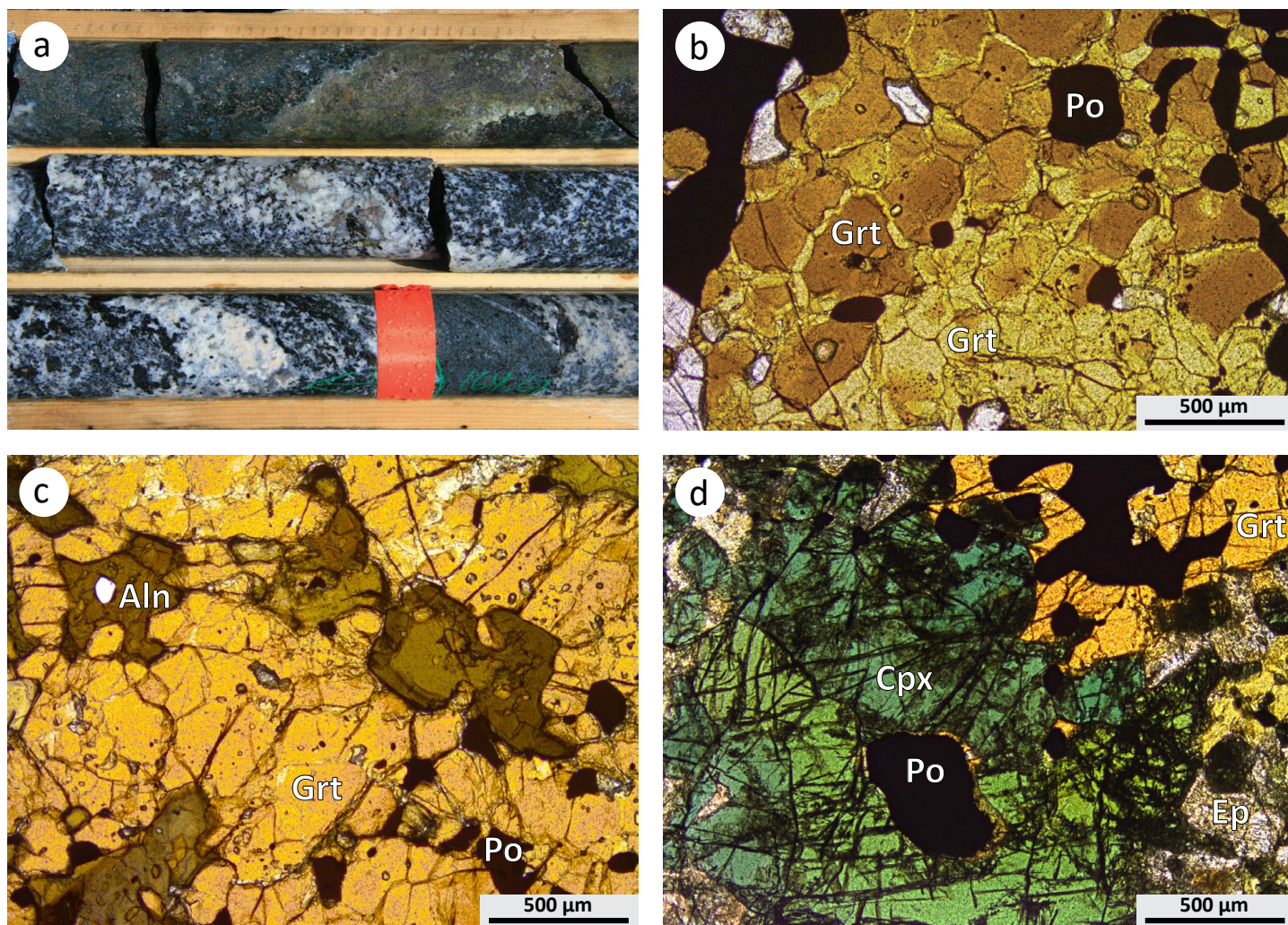


Figure 10: Drillcore and thin section images of sulphide-rich calcsilicate: **a)** sulphide-rich calcsilicate (top row) and foliated tonalite (bottom two rows; 167.7 m); **b)** photomicrograph in PPL of yellow- to brown-zoned garnet and pyrrhotite, which are the most abundant minerals in the sulphide-rich calcsilicate; **c)** photomicrograph in PPL of zoned allanite and garnet; **d)** photomicrograph in PPL of the clinopyroxene-rich selvage to the sulphide-rich calcsilicate. Abbreviations: Aln, allanite; Cpx, clinopyroxene; Ep, epidote; Grt, garnet; Po, pyrrhotite.

employ a lithium metaborate/tetraborate fusion technique, followed by nitric-acid digestion and analysis by inductively coupled plasma–optical emission spectrometry (ICP-OES) for the major elements and selected trace elements (Ba, Be, Sc, Sr, V, Y, Zr), and inductively coupled plasma–mass spectrometry (ICP-MS) for the remainder of the trace elements and REE. Additional analysis by ion-specific electrode (ISE) for F was conducted on one sample of calcsilicate and two samples of quartz monzonite. Samples of the calcsilicate and quartz monzonite were analyzed by total-digestion ICP-OES for selected trace elements (Ag, Cd, Cu, Ni, Pb, Zn) and sulphur contained within sulphides. Samples of the sulphide- and titanite-rich calcsilicate were also analyzed for carbon and sulphur, through induction-furnace combustion and measurement of the release of CO₂ and SO₂ by infrared spectrometry.

Granitoid rocks

The foliated quartz monzodiorite, quartz monzonite, and majority of foliated tonalite samples are metaluminous, while the various granites are peraluminous (Figure 12). The Mg# val-

ues (molar Mg/Mg+Fe) for the monzodiorite, monzonite, and tonalite are relatively intermediate and range from 0.40 to 0.51. The foliated granite and pegmatitic granite have Mg# values of 0.39 and 0.37, respectively, and the aplitic granite and massive granite are relatively iron-rich with Mg# values of 0.18–0.21.

Chondrite-normalized REE profiles of the majority of granitoids have moderate negative slopes ($[La/Lu]_N = 32\text{--}110$; Figure 13a–d). The REE profiles of the foliated tonalite, foliated monzodiorite, and foliated granite are characterized by positive Eu anomalies ($Eu/Eu^* = 1.29\text{--}1.30$, 1.86, and 2.47, respectively). The profiles of the aplitic granite are characterized by weak negative Eu anomalies ($Eu/Eu^* = 0.60\text{--}0.62$), while the massive granite profiles are characterized by little to no anomaly at Eu. The normalized REE profiles of the quartz monzonite are distinctly steeper ($[La/Lu]_N = 85\text{--}480$; Figure 13e) with variable Eu anomalies ($Eu/Eu^* = 0.93\text{--}1.91$). The pegmatitic granite is characterized by the steepest negative REE profile ($[La/Lu]_N = 2800$; Figure 13f) and a pronounced positive Eu anomaly ($Eu/Eu^* = 2.25$).

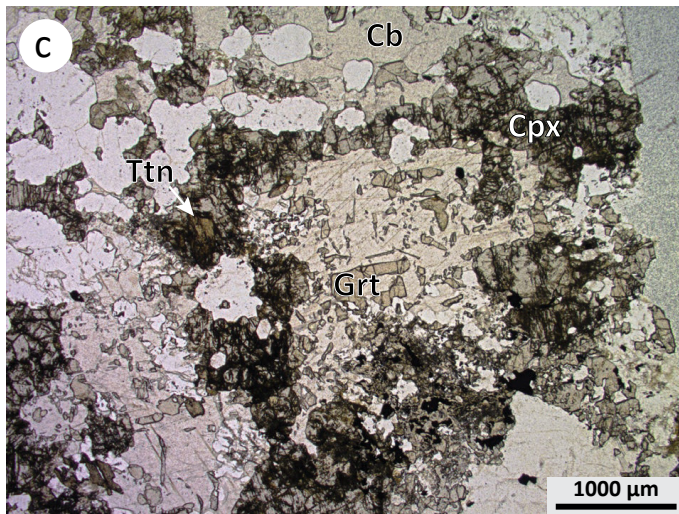
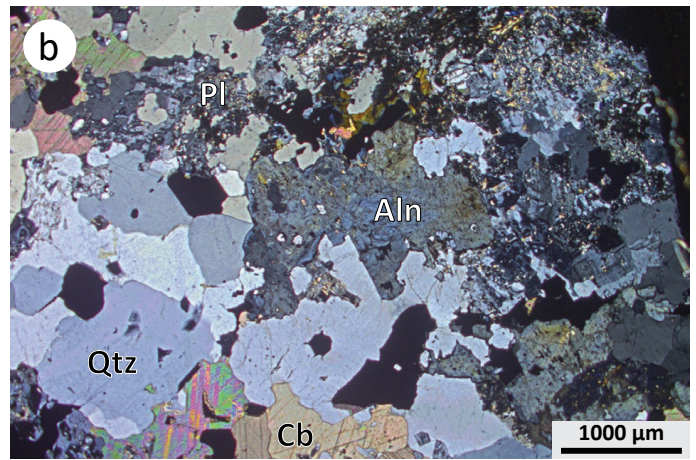
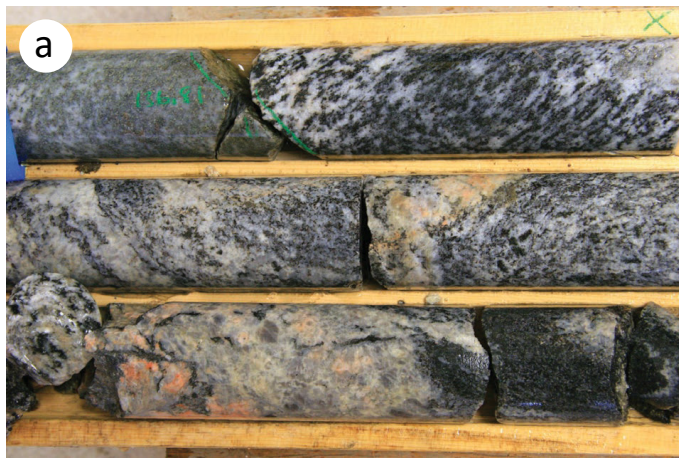


Figure 11: Drillcore and thin section images of the bleached tonalite: **a)** bleached tonalite (top row, left of green wax pencil line) crosscutting foliated tonalite (right of wax pencil line); **b)** photomicrograph in XPL of allanite and recrystallized felted plagioclase in groundmass; **c)** photomicrograph in PPL of relict garnet enclosed by carbonate with a clinopyroxene corona. Abbreviations: Aln, allanite; Cb, carbonate; Cpx, clinopyroxene; Grt, garnet; Pl, plagioclase; Qtz, quartz; Ttn, titanite.

Table 1: Summary of lithogeochemical results for representative samples of granitoids, sulphide- and titanite-rich calcsilicate, and bleached tonalite from the Huzyk Creek property.

	Fol tonalite	Fol Qtz Mzdr	Fol granite	Quartz monzonite			Aplitic granite	Massive granite	Peg granite	Sulphide- and titanite-rich calcsilicate			Bleached Rk
Sample	108-20-HZ10	108-20-HZ13	108-20-HZ16	108-20-HZ03	108-20-HZ09	108-20-HZ22 ⁽¹⁾	108-20-HZ04	108-20-HZ19	108-20-HZ15	108-20-HZ02	108-20-HZ08	108-20-HZ11	108-20-HZ07
Lithology	Tonalite	Qtz Mzdr	Granite	Monzonite	Granite	Quartz Mz	Granite	Granite	Granite	Disc Calcsil	Fol Calcsil	Su-rich Calcsil	Altered Tn
wt. %													
SiO ₂	60.09	56.4	63.24	59.32	64.74	61.28	72.27	72.04	67.54	51.94	45.73	12.69	56.55
Al ₂ O ₃	16.66	16.88	15.79	19.48	16.12	16.21	13.26	13.63	15.7	14.72	11.95	2.41	14.43
Fe ₂ O ₃	5.99	6.21	3.64	2.33	2.4	3.07	1.66	2.21	1.78	8.36	13.61	61.39	6.52
MnO	0.079	0.116	0.026	0.029	0.031	0.048	0.018	0.024	0.017	0.086	0.214	0.044	0.083
MgO	2.94	2.86	1.16	1.08	0.81	1.14	0.22	0.29	0.52	3.92	4.33	0.48	2.28
CaO	5.46	7.34	2.5	4.58	2.9	4.14	1.18	1.37	0.77	8.75	16.08	14.63	8.46
Na ₂ O	4.71	3.91	3.57	4.51	3.09	3.4	3.26	3.42	2.35	3.53	2.15	0.03	2.73
K ₂ O	1.82	2.97	4.52	5.21	6.3	5.37	5.31	4.71	8.44	1.73	0.5	<0.01	2.63
TiO ₂	0.793	1.278	1.305	0.426	0.596	1.473	0.112	0.195	0.412	0.689	2.159	0.648	0.404
P ₂ O ₅	0.31	0.32	0.29	0.29	0.25	0.45	0.03	0.03	0.07	0.69	0.3	0.48	0.59
LOI	1.4	1.54	1.43	1.48	1.23	1.56	1.19	0.59	0.99	3.5	2.82	4.7	2.27
Total	100.2	99.82	97.48	98.73	98.47	98.15	98.51	98.52	98.59	97.9	99.86	97.51	96.96
C	na.	na.	na.	na.	na.	0.24	na.	na.	na.	0.12	0.53	0.63	0.55
S	na.	0.17	na.	0.14	0.05	0.07	na.	na.	na.	3.24	0.79	19.30	1.82

⁽¹⁾ Re-analysis of 108-19-HZ22 (Couëslan, 2020b).

Abbreviations: ASI, aluminum saturation index; bdl., below detection limit; Calcsil, calcsilicate; Disc, discordant; Fol, foliated; LOI, loss-on-ignition; Mz, monzonite; Mzdr, monzodiorite; na., not analyzed; Peg, pegmatite; Qtz, quartz; Rk, rock; Su, sulphide; Tn, tonalite.

Table 1 (continued): Summary of lithogeochemical results for representative samples of granitoids, sulphide- and titanite-rich calcsilicate, and bleached tonalite from the Huzyk Creek property.

Sample Lithology	Fol tonalite	Fol Qtz Mzdr	Fol granite	Quartz monzonite			Aplitic granite	Massive granite	Peg granite	Sulphide- and titanite-rich calcsilicate			Bleached Rk
	108-20- HZ10 Tonalite	108-20- HZ13 Qtz Mzdr	108-20- HZ16 Granite	108-20- HZ03 Monzonite	108-20- HZ09 Granite	108-20- HZ22 ⁽¹⁾ Quartz Mz	108-20- HZ04 Granite	108-20- HZ19 Granite	108-20- HZ15 Granite	108-20- HZ02 Disc Calcsil	108-20- HZ08 Fol Calcsil	108-20-HZ11 Su-rich Calcsil	108-20- HZ07 Altered Tn
(ppm)													
Sc	12	15	2	9	4	5	2	2	2	13	36	4	9
V	109	149	81	41	52	89	bdl.	8	34	107	438	150	76
Ba	1730	6271	11190	11630	16860	14530	1432	2092	16570	5532	414	32	7675
Sr	1093	2757	1994	3879	4219	3697	282	413	1367	4022	394	1279	5849
Y	9	12	6	16	7	35	5	3	3	34	38	26	17
Zr	136	139	787	240	367	1143	83	124	92	54	131	55	196
Ni	30	35	bdl.	4	3	3	bdl.	bdl.	bdl.	53	39	213	25
Cu	bdl.	53	bdl.	47	35	20	bdl.	bdl.	20	490	110	1930	245
Ga	21	19	18	24	17	19	16	16	16	20	19	24	20
Rb	27	31	57	42	55	44	90	79	87	18	6	bdl.	21
Nb	5	9	7	4	3	11	3	3	2	10	10	3	3
La	56	67.1	87.4	589	188	253	48.3	64.1	271	264	31.2	363	411
Ce	111	136	169	1020	311	634	83.2	108	448	630	66.4	729	726
Pr	12.4	16.8	19.5	102	30	83.5	8.4	10.2	42.8	85.2	8.3	96.7	76.3
Nd	44.5	64.2	71.7	323	94	323	27.2	30.5	128	354	33.3	368	257
Sm	6	9.5	8.8	30.8	8.8	44.6	3.7	3.3	9.5	53.3	7.1	46.9	28.2
Eu	2.16	4.69	5.43	7.04	4.24	11.8	0.6	0.81	5.05	10.7	2.25	10.3	7.24
Gd	3.7	5.1	3.7	12.3	3.9	20.5	1.9	1.4	3.1	24.9	6.8	21.5	12.2
Tb	0.4	0.5	0.3	1	0.3	1.9	0.2	0.2	0.2	2.2	1.1	2	1
Dy	2.1	2.6	1.5	4.1	1.3	8	0.9	0.6	0.5	8.6	7.2	7.9	3.9
Ho	0.4	0.4	0.3	0.5	0.2	1.4	0.2	0.1	bdl.	1.3	1.5	1.1	0.6
Er	1	0.9	0.8	1.2	0.5	3.3	0.5	0.4	0.1	3	4.1	2.6	1.1
Tm	0.14	0.13	0.09	0.16	0.07	0.42	0.07	0.06	bdl.	0.37	0.6	0.3	0.14
Yb	0.9	0.9	0.6	1	0.4	2.2	0.5	0.4	bdl.	2	4.1	1.5	1
Lu	0.12	0.16	0.09	0.15	0.08	0.31	0.06	0.06	0.01	0.27	0.61	0.19	0.14
Hf	3.2	3	12.7	5	6.6	18.4	2.4	3.3	1.6	1.6	3.6	1.4	3.9
Ta	0.1	0.2	0.2	0.2	bdl.	0.6	0.1	bdl.	bdl.	0.5	0.6	0.2	<0.1
Th	0.4	0.9	2.1	35.4	10.3	11.6	18.6	15.7	24.1	11.1	2.2	9.3	9.9
U	0.4	0.6	1.2	1.5	0.7	2.8	3.7	2.5	0.9	3.3	1.1	3.2	1.6
Mg#	0.49	0.48	0.39	0.48	0.40	0.42	0.21	0.21	0.37	0.48	0.39	0.02	0.41
ASI	0.85	0.73	1.03	0.91	0.94	0.86	1.00	1.03	1.09	0.62	0.36	0.09	0.64
(La/Lu) _N	48.4	43.5	101	408	244	84.7	83.6	111	2813	101	5.31	198	305
Eu/Eu*	1.30	1.85	2.47	0.93	1.91	1.04	0.62	0.98	2.25	0.78	0.97	0.86	1.02

⁽¹⁾ Re-analysis of 108-19-HZ22 (Couëslan, 2020b).

Abbreviations: ASI, aluminum saturation index; bdl., below detection limit; Calcsil, calcsilicate; Disc, discordant; Fol, foliated; LOI, loss-on-ignition; Mz, monzonite; Mzdr, monzodiorite; na., not analyzed; Peg, pegmatite; Qtz, quartz; Rk, rock; Su, sulphide; Tn, tonalite.

Primitive mantle-normalized multi-element diagrams of the granitoids are characterized by negative slopes with depletions at Nb and Ti (Figure 14). Barium is strongly enriched in the foliated monzodiorite, foliated granite, quartz monzonite, and pegmatitic granite. Thorium is relatively depleted in the foliated tonalite, foliated monzodiorite, and foliated granite. Depletions are also present at Zr in the profiles of the monzodiorite, monzonite, and

aplitic and pegmatitic granites. Zirconium is enriched in the profile of the foliated granite.

Calcsilicate and bleached tonalite

The major-element chemistry of the calcsilicate varies depending on the sulphide content with SiO₂ values ranging from 12.7% in the most sulphide-rich sample to 51.9% in a sample

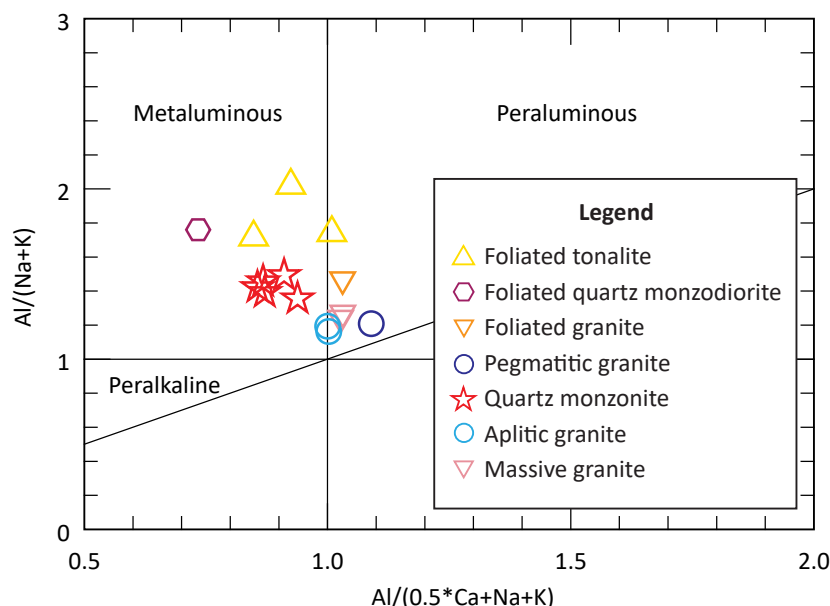


Figure 12: The composition of Huzyk Creek granitoids plotted on the alumina saturation index diagram of Maniar and Piccoli (1989).

containing minor sulphide. There is a similar inverse relationship between alumina-saturation indices (0.09–0.69) and Mg# values (0.02–0.53) relative to sulphide content. The bleached tonalite contains 56.5% SiO₂ with an aluminum saturation index of 0.64 and Mg# of 0.41.

The trace-element chemistry of the calcsilicates is also variable, but not correlative with the sulphide content. Chondrite-normalized REE profiles reveal two groups, one is relatively depleted with shallow negative slopes ($[La/Lu]_N = 3.1–5.3$; Figure 15a), and comprises the semiconcordant calcsilicate and foliated, titanite-rich calcsilicate. The other group is enriched with steep negative slopes ($[La/Lu]_N = 101–198$; Figure 15b), and includes the discordant calcsilicate and the sulphide-rich calcsilicate. The primitive mantle-normalized multi-element profiles of the depleted calcsilicate are characterized by slight depletions at Nb, Zr and Ti (Figure 15c), while the enriched calcsilicate profiles are characterized by pronounced depletions of the same elements (Figure 15d). Strontium is enriched in one sample of depleted calcsilicate, but is typically depleted in other calcsilicate samples. The sulphide-rich calcsilicate is depleted in Ba. The REE and multi-element profiles of the bleached tonalite are similar to the enriched calcsilicate. The enriched calcsilicate and bleached tonalite contain higher concentrations of S than the depleted calcsilicate (Table 1).

Radiogenic isotope analyses

One sample of quartz monzonite (108-20-HZ03) was submitted for whole-rock Sm-Nd isotope geochemistry and zircon U-Pb geochronology. The sample is a massive clinopyroxene-bearing monzonite and is interpreted as a least altered/metasomatized example of the quartz monzonite suite. Results for the zircon U-Pb geochronology can be found in Table 2, and results for the whole-rock Sm-Nd isotope geochemistry are published in Manitoba Geological Survey (2021) and summarized in Table 3.

Zircon U-Pb geochronology

The sample was submitted to the Jack Satterly Geochronology Laboratory at the University of Toronto (Toronto, Ontario) for isotope dilution–thermal ionization mass spectrometry (ID-TIMS). It was reduced in size using a conventional jaw crusher, followed by grinding to a coarse powder using a hardened steel disk mill. An initial heavy mineral separate was created by passing the comminuted sample several times over a Wilfley table. The heavy mineral separate was further processed by density separations with methylene iodide and magnetic separations with a Frantz isodynamic separator. As a final step, the freshest, least cracked, core- and inclusion-free grains of zircon were hand picked in alcohol under a binocular microscope from the least magnetic separate.

The highest quality zircon grains were annealed in quartz crucibles at 900 °C for 2 days (procedure modified after Mattinson, 2005) to remove radiation damage prior to chemical abrasion. The annealed grains were subsequently etched in approximately 0.10 ml of concentrated HF for several hours in Teflon™ vessels at 195 °C in order to remove altered domains, which may contain isotopically disturbed Pb. Chemically abraded zircon fractions were washed and sonicated in 7N HNO₃ for approximately 30 minutes prior to dissolution. A mixed ²⁰⁵Pb–²³⁵U isotopic spike was added to the dissolution capsules during sample loading. Zircon was then completely dissolved using concentrated HF in Teflon bombs at 195 °C for 3–4 days, then dried and re-dissolved in 3N HCl overnight (Krogh, 1973). Uranium and Pb were isolated using 50 µl anion exchange columns using HCl elutions, dried down, and then loaded onto outgassed zone-refined rhenium filaments with silica gel (Gerstenberger and Haase, 1997).

Lead and UO₂ were analyzed on a VG354 mass spectrometer using a Daly collector in pulse counting mode. The mass discrimination correction for the detector was constant at 0.07%/amu. Thermal mass discrimination corrections are 0.10%/amu for Pb

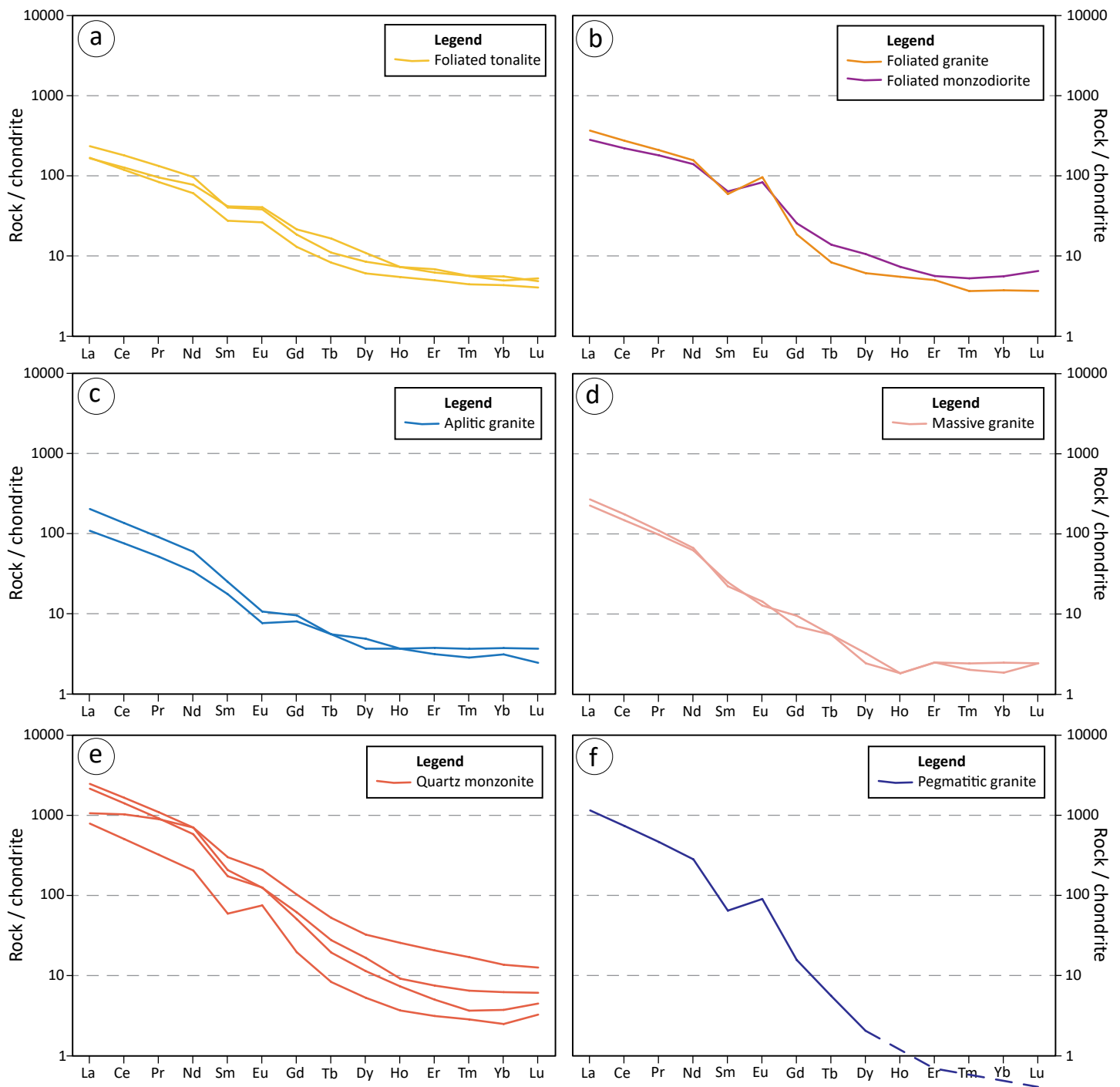


Figure 13: Chondrite-normalized rare-earth element profiles of Huzyk Creek granitoids: **a)** foliated tonalite; **b)** foliated monzodiorite and foliated granite; **c)** aplitic granite; **d)** massive granite; **e)** quartz monzonite; **f)** pegmatitic granite. Dashed lines connect points that are separated by no data, which is the result of element concentrations below the detection limit of the analytical technique. Chondrite values are from McDonough and Sun (1995).

and U. Deadtime of the Daly system was 18 ns for Pb during the analytical period, monitored using the SRM982 Pb standard. Mass spectrometer data was reduced using in-house software (UtilAge program) coded by D. Davis. Corrections for initial ^{230}Th disequilibrium in zircon were applied to the $^{206}\text{Pb}/^{238}\text{U}$ ages, assuming a Th/U ratio in the magma of 4.2. All common Pb was assigned to procedural blank. Initial Pb from geological sources above 1 pg was corrected using the Pb evolution model of Stacey and Kramers (1975). Concordia diagram and mean age were

calculated using the Isoplot version 3.75 Add-In for Microsoft® Excel® of Ludwig (2012).

Sample 108-20-HZ03 yielded relatively coarse-grained zircon (up to ~500 μm ; Figure 16a). The grains are pale yellow to colourless, generally irregular in form, and lack well-developed crystal faces. Rare, broken subhedral to euhedral 3:1 forms are present. Only minor cracks and inclusions occur. Six single grain fractions (Figure 16b) yielded concordant or near concordant U-Pb ages arrayed along concordia from 1808.1 to 1799.6 Ma (Figure 16c).

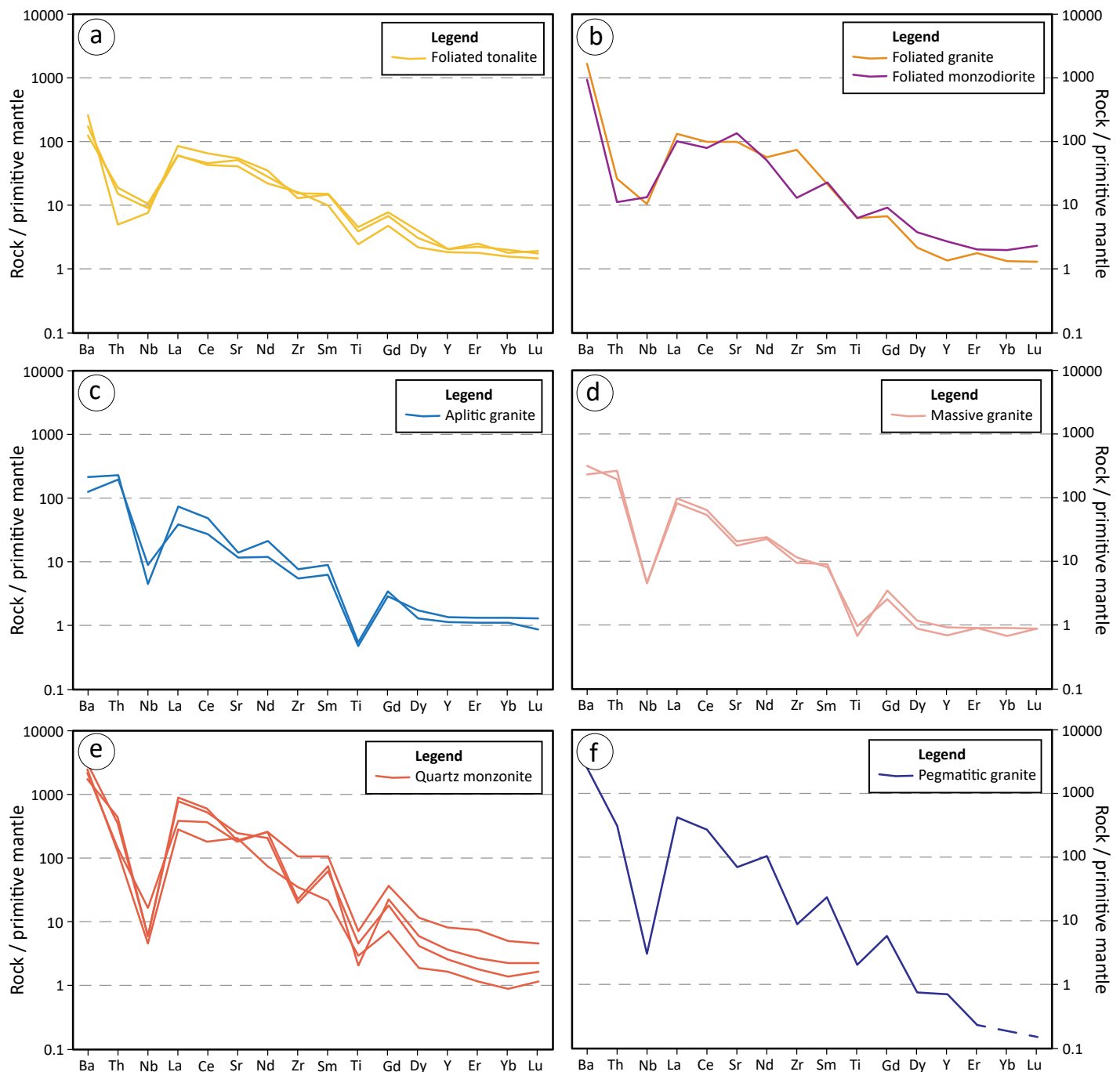


Figure 14: Primitive mantle-normalized multi-element profiles of granitoid rocks from the Huzyk Creek drillcore: **a)** foliated tonalite; **b)** foliated monzodiorite and foliated granite; **c)** aplitic granite; **d)** massive granite; **e)** quartz monzonite; **f)** pegmatitic granite. Dashed lines connect points that are separated by no data, which is the result of element concentrations below the detection limit of the analytical technique. Primitive mantle values are from McDonough and Sun (1995).

The dispersion of data can be interpreted in at least two ways. The most straightforward interpretation is that the two youngest fractions (Z2 and Z6) represent the magmatic age. The age of these fractions overlap and share a unique Th/U ratio (0.33) relative to the other analyses (Table 2). The two youngest fractions yield a mean concordia age of 1800.5 ± 2.4 Ma (at 2σ ; Figure 16d). In this scenario, the older analyses would reflect minor inheritance from older phases of the monzonite complex or the adjacent country rock.

An alternative interpretation is that the two oldest age fractions represent the magmatic age. Fractions Z1 and Z4 overlap within error but have significantly different Th/U ratios of 0.40 and 0.27, respectively (Table 2). The two oldest fractions yield a mean concordia age of 1806.8 ± 6.4 Ma (at 1.96σ ; Figure 16d). In this scenario, the younger age fractions could be an artefact of secondary Pb-loss during metamorphism, possibly near 1800 Ma. There are two lines of evidence that argue against this latter interpretation:

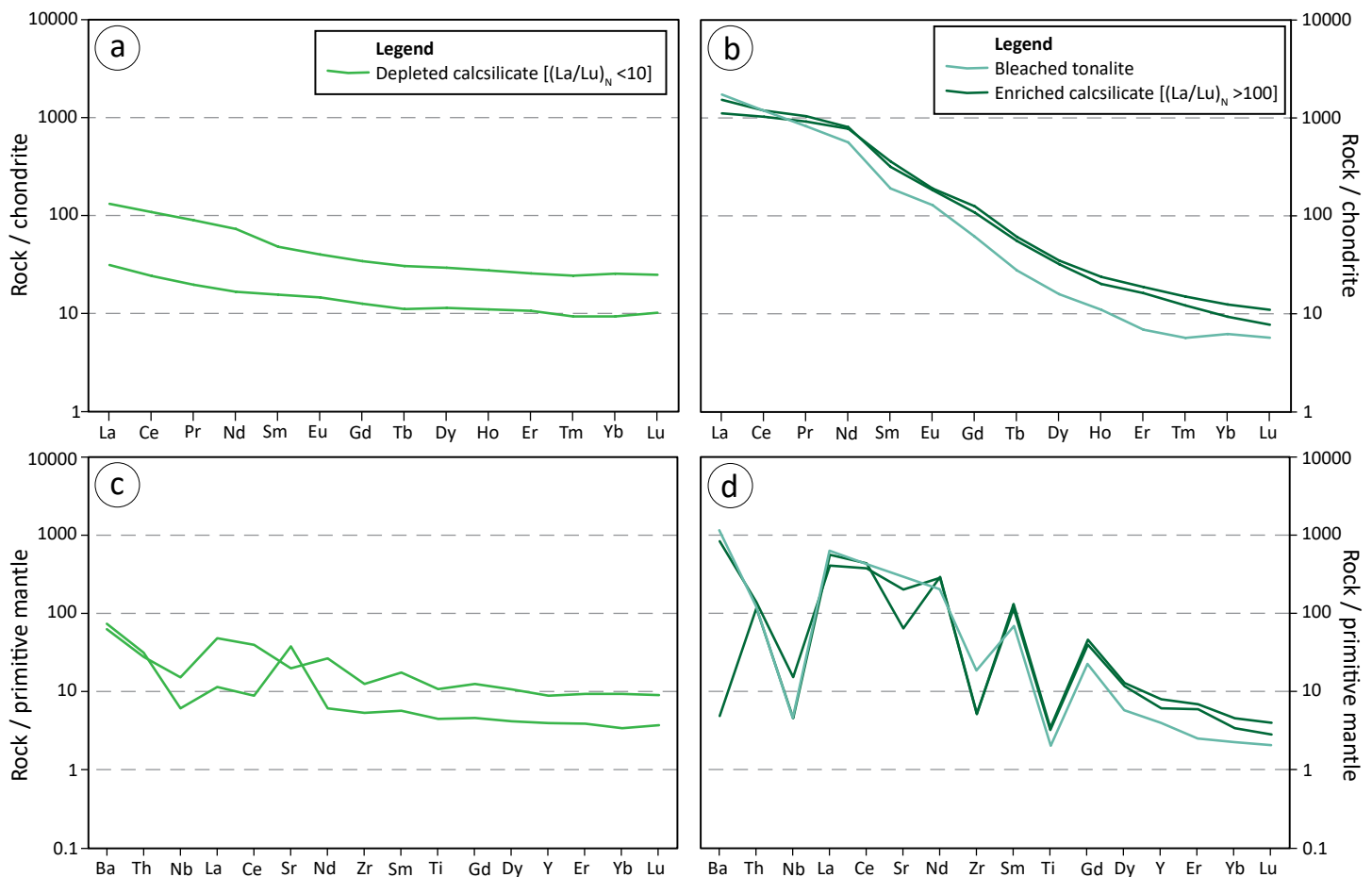


Figure 15: Geochemical diagrams for the sulphide- and titanite-enriched calcsilicate and bleached tonalite: **a)** chondrite-normalized REE profiles of the depleted calcsilicate; **b)** chondrite-normalized REE profiles of the enriched calcsilicate and bleached tonalite; **c)** primitive mantle-normalized multi-element profiles of the depleted calcsilicate; **d)** primitive mantle-normalized multi-element profiles of the enriched calcsilicate and bleached tonalite. Chondrite and primitive mantle values are from McDonough and Sun (1995).

- 1) Peak metamorphic assemblages in the Huzyk Creek area are of the lower granulite-facies and characterized by a well developed foliation (Couëslan, 2020a), but sample 108-20-HZ03 is massive suggesting it post-dates peak metamorphism.
- 2) There is no systematic decrease in Th/U ratios from higher igneous values in the oldest fractions to lower metamorphic values in the younger fractions; in fact, there appears to be an increase in Th/U ratios towards the younger fractions (Figure 16e; Table 2).

Whole-rock Sm-Nd isotope geochemistry

Sample 108-20-HZ03 was submitted for Sm-Nd isotope geochemical analysis to the University of Alberta Radiogenic Isotope Facility (Edmonton, Alberta). Initial sample preparation followed the same procedures as outlined for the lithochemical analysis. The sample was processed and analyzed for Sm-Nd isotopes following the chromatographic and mass-spectrometry methods outlined by Unterschutz et al. (2002) and Schmidberger et al. (2007). The Sm and Nd isotopic composition was determined by multicollector ICP-MS, for which an in-house Nd isotope standard was used (Schmidberger et al., 2007). Chemical processing blanks

were <200 pg for Nd and Sm. The Nd data is presented relative to a $^{143}\text{Nd}/^{144}\text{Nd}$ value of 0.511850 for the La Jolla standard.

A crustal residence model age (T_{CR}) of ca. 2.03 Ga was calculated based on the model of Goldstein et al. (1984; Table 3), which assumes a linear evolution of isotopic ratios in the depleted mantle, using present-day depleted-mantle values of $^{143}\text{Nd}/^{144}\text{Nd} = 0.513160$ and $^{147}\text{Sm}/^{144}\text{Nd} = 0.2141$. An initial ϵ_{Nd} value of +1.7 was calculated using a crystallization age of 1.80 Ga.

Discussion

The relative timing of intrusion of the granitoid phases can be broadly divided based on the presence or absence of a well-developed foliation. In this scheme we have an older group of intrusions including the foliated tonalite, foliated quartz monzoniorite, and the foliated granite, and a younger group of intrusions consisting of the quartz monzonite and massive granite. There are likely several generations of pegmatitic granite and aplitic granite in the drillcore; however, the collected samples consist of a foliated pegmatite, which can be assigned to the older suite of intrusions, and non-foliated aplite, which can be assigned to the younger suite.

Table 2: U-Pb ID-TIMS analytical data for zircon fractions from quartz monzonite sample 108-20-HZ03.

Fraction	Description ⁽¹⁾	U (ppm)	Th/U	Pb ^T (pg)	²⁰⁴ Pb (pg)	Isotopic ratios ⁽²⁾								Ages ⁽²⁾ (Ma)						
						²⁰⁶ Pb/ ²⁰⁴ Pb	²⁰⁷ Pb/ ²³⁵ U	±2s	²⁰⁶ Pb/ ²³⁸ U	±2s	Corr coeff (ρ)	²⁰⁷ Pb/ ²⁰⁶ Pb	±2s	²⁰⁷ Pb/ ²³⁵ U	±2s	²⁰⁶ Pb/ ²³⁸ U	±2s	²⁰⁷ Pb/ ²⁰⁶ Pb	±2s	Disc (%)
Z1	lrg, gl-clr, cls shard	432	0.397	557	0.19	182637	4.93342	0.01131	0.323863	0.000616	0.9407	0.110481	0.000090	1808.0	1.9	1808.6	3.0	1807.3	1.5	−0.1
Z2	med, gl-clr, cls shard	301	0.329	368	0.12	196270	4.89348	0.01111	0.322298	0.000605	0.9381	0.110118	0.000091	1801.1	1.9	1800.9	2.9	1801.4	1.5	0.0
Z3	lrg, gl-clr, cls, brkn el pr	270	0.295	222	0.76	18253	4.90596	0.01180	0.322802	0.000644	0.9403	0.110227	0.000095	1803.3	2.0	1803.4	3.1	1803.1	1.6	−0.0
Z4	med, gl-clr, cls, blocky frag	320	0.265	409	1.42	18076	4.91671	0.01388	0.322623	0.000805	0.9490	0.110530	0.000100	1805.1	2.4	1802.5	3.9	1808.1	1.7	0.4
Z5	lrg, gl-clr, cls, brkn el frag	629	0.232	893	0.20	276542	4.91690	0.01194	0.323299	0.000667	0.9463	0.110302	0.000090	1805.2	2.0	1805.8	3.2	1804.4	1.5	−0.1
Z6	lrg, gl-clr, cls, brkn el pr	388	0.334	665	0.42	97555	4.88654	0.01270	0.322160	0.000726	0.9528	0.110009	0.000090	1799.9	2.2	1800.3	3.5	1799.6	1.5	−0.0

⁽¹⁾ Analyses of single grain fractions.⁽²⁾ Isotopic ratios and ages are corrected for fractionation, blank, spike, and initial common Pb (Stacey and Kramers, 1975).Abbreviations: brkn, broken; clr, clear; cls, colourless; coeff, coefficient; Corr, correlation; Disc, discordance; el, elongate; frag, fragment; gl, glassy; lrg, large; med, medium; Pb^T, total Pb; pg, picograms; pr, prism.

Table 3: Summary of Sm-Nd isotopic data for quartz monzonite sample 108-20-HZ03 (Manitoba Geological Survey, 2021).

Sample number	Rock type	Sm (ppm)	Nd (ppm)	¹⁴⁷ Sm/ ¹⁴⁴ Nd ⁽¹⁾	¹⁴³ Nd/ ¹⁴⁴ Nd ⁽²⁾	εNd ⁽³⁾ (1.80 Ga)	T _{CR} ⁽⁴⁾ (Ga)
108-20-HZ03	Quartz monzonite	31.1	322	0.0584	0.511084 (8)	1.7	2.03

⁽¹⁾ Estimated error is better than 0.5%.
⁽²⁾ Presented relative to ¹⁴³Nd/¹⁴⁴Nd = 0.511850 for the La Jolla standard; numbers in parentheses are the 2σ uncertainties × 10⁻⁶.
⁽³⁾ ε_{Nd} values at 1.80 Ga calculated using present-day chondritic ratios of ¹⁴³Nd/¹⁴⁴Nd = 0.512638 and ¹⁴⁷Sm/¹⁴⁴Nd = 0.1967.
⁽⁴⁾ Crustal residence Nd model ages (T_{CR}) calculated according to the linear model of Goldstein et al. (1984).

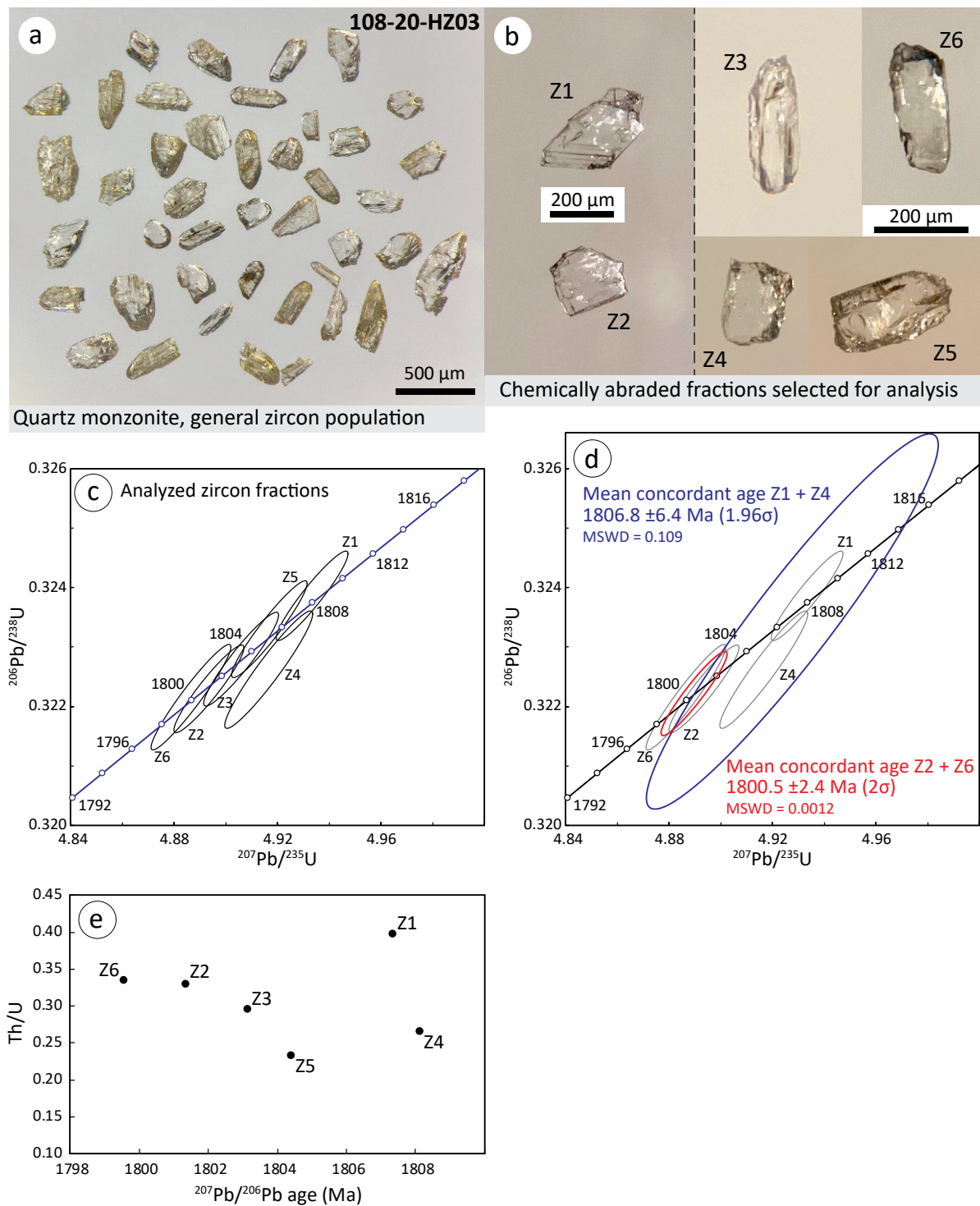


Figure 16: Zircon separates, fractions, and ID-TIMS results for sample 108-20-HZ03: **a)** zircon separate recovered from sample; **b)** chemically abraded zircon fractions selected for ID-TIMS analysis; **c)** U-Pb concordia diagram for analyzed zircon fractions; **d)** mean concordant ages for zircon fractions Z2 + Z6 (at 2σ) and Z1 + Z4 (at 1.96σ); **e)** Th/U ratios of zircon fractions. Error ellipses are shown at 2σ. Abbreviation: MSWD, mean square of weighted deviates.

Within these two groups there are also distinct geochemical trends which can be identified from whole-rock major-element and trace-element geochemistry. The foliated tonalite plots within the calcalkaline-series field of the K_2O - SiO_2 diagram of Peccerillo and Taylor (1976), while the foliated monzodiorite and foliated granite plot within the high-K calcalkaline field (Figure 17). The foliated pegmatitic granite plots in the shoshonite field. Within the younger suite of intrusions, the aplitic granite and massive granite form a cluster of points in the calcalkaline field and the quartz monzonite forms a broadly distributed series of points in the shoshonite field.

Normalized REE and multi-element profiles of the foliated granitoids also reveal differences between the subdivisions. Barium and LREE becoming increasingly enriched from the calcalkaline tonalite to the high-K calcalkaline monzodiorite and granite to the pegmatitic granite (Figure 18). It is also noted that although the pegmatitic granite plots within the shoshonitic field of Figure 17, the REE and multi-element profiles are distinctly different from the profiles of the quartz monzonite. Profiles of the massive granite and the aplitic granite are similar, with the massive granite having slightly steeper REE profiles and little to no anomalies at Eu and Zr (Figure 19). The profiles of the massive and aplitic granites are distinctly different from that of the quartz monzonite.

The granitoids typically plot within the volcanic-arc and syn-collisional granitoid fields of discrimination diagrams (Figure 20); however, the quartz monzonite data plots, at least in part, within the A-type granitoid fields in the Zr-Ga/Al diagram of Whalen et al. (1987) and in the sliding normalization diagram of Liégeois et al. (1998; Figure 20b, c). This appears to be a function of the high concentrations of Zr and LREE within the monzonite, which are

characteristic of A-type granitoids. Other characteristics of A-type granitoids include high alkalis, Nb, Ga and total REE (except Eu), and low Ca, Ba, Sr, Eu, Mg#, Sc and V (Whalen et al., 1987; Eby, 1990; King et al., 1997; Bonin, 2007). Many of these characteristics are in contrast with the monzonite which is strongly enriched in Ba and Sr (11630–20350 ppm and 3697–5016 ppm, respectively), contains significant CaO (2.90–4.58 wt. %), has intermediate Mg# values (0.40–0.48), is depleted in Nb (3–11 ppm) and HREE ($[La/Lu]_N = 85$ –480), and can be enriched in Eu ($Eu/Eu^* = 0.93$ –1.91; Figure 21). Therefore, the Huzyk Creek quartz monzonite does not appear to be an A-type granitoid.

Syenite intrusions from the Paint Lake area of the Thompson nickel belt share some geochemical similarities (Figures 1, 22). They are enriched in Ba and Sr (4370–5370 ppm and 1220–1479 ppm, respectively), contain significant CaO (1.97–3.04 wt. %), and are depleted in Nb (11–27 ppm) and HREE ($[La/Lu]_N = 97$ –122) with little to no depletion of Eu ($Eu/Eu^* = 0.81$ –0.92; Figure 23; Couëslan, 2016). However, the Paint Lake intrusions are texturally distinct with large K-feldspar phenocrysts in a mafic-rich groundmass, and they are geochemically primitive with relatively high Mg# values (0.74–0.76) and enrichment in Cr and Ni (328–437 ppm and 218–269 ppm, respectively). The Paint Lake intrusions are also older (ca. 1880 Ma) and more isotopically evolved ($\epsilon Nd = -14.4$ to -15.0 at 1.88 Ga; Couëslan, 2016) than the Huzyk Creek quartz monzonite.

The geochemical characteristics of the Huzyk Creek quartz monzonite is more comparable to the high-K calcalkaline to shoshonitic intrusions of the Trans-Hudson orogen of Manitoba such as at Eden, Burntwood, and Brezden lakes, and along the Suwannee River (Figures 1, 22; Chakhmouradian et al., 2008; Martins et al., 2011, 2012a; Martins and Couëslan, 2022). These intrusions

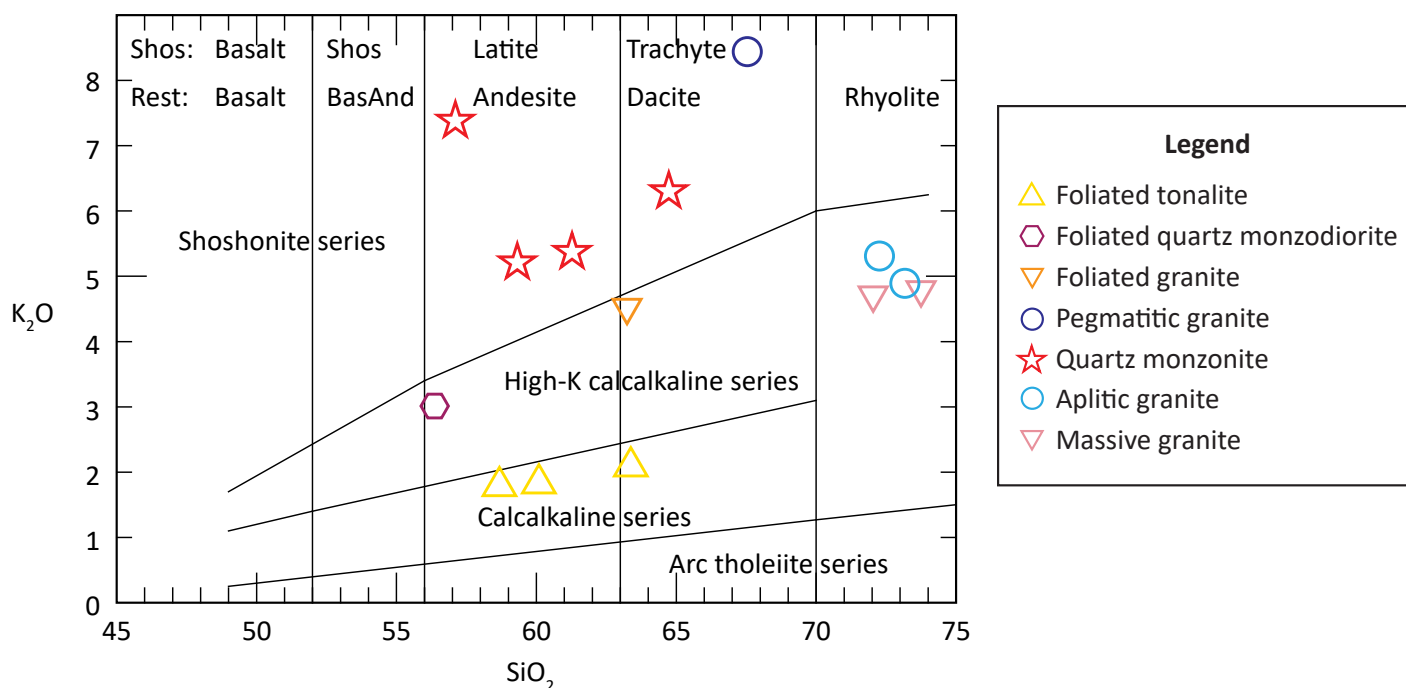


Figure 17: K_2O - SiO_2 diagram of Peccerillo and Taylor (1976) showing the composition of Huzyk Creek granitoids. Abbreviations: BasAnd, basaltic andesite; Shos, shoshonite/shoshonite series.

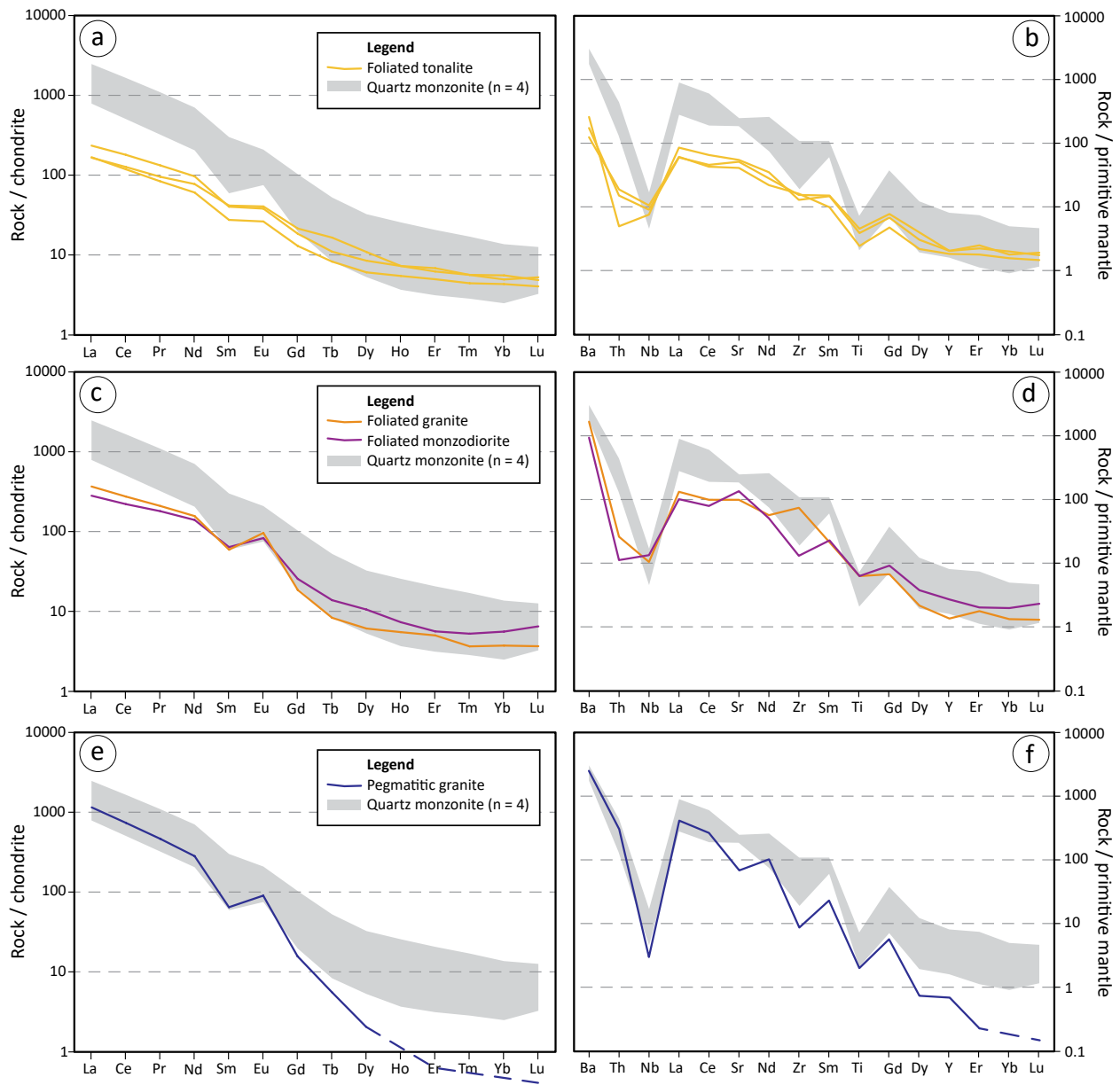


Figure 18: Chondrite-normalized REE profiles (left column) and primitive mantle-normalized multi-element profiles (right column) of the foliated granitoids compared to the quartz monzonite. Chondrite and primitive mantle values are from McDonough and Sun (1995).

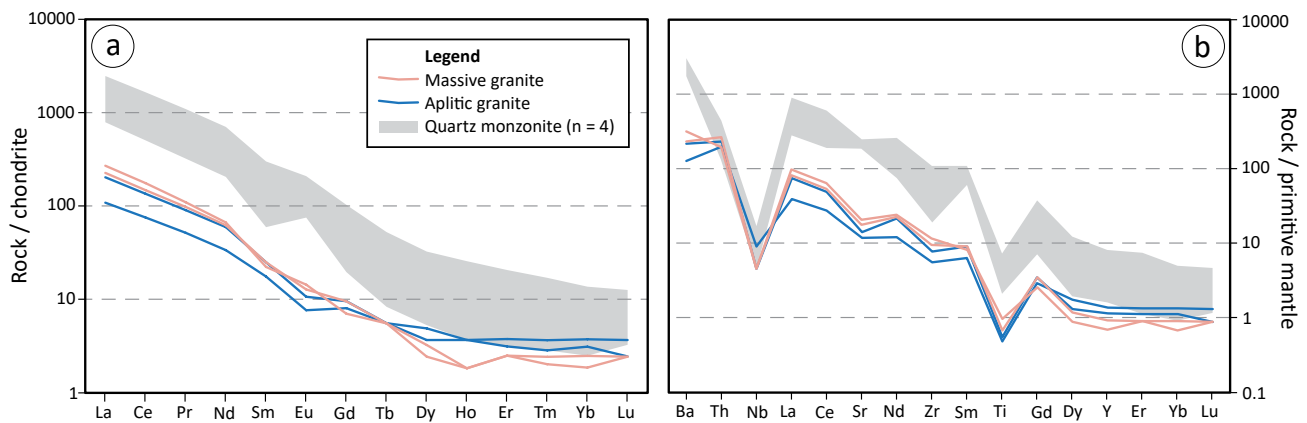


Figure 19: Chondrite-normalized REE profiles (a) and primitive mantle-normalized multi-element profiles (b) of the massive granitoids compared to the quartz monzonite. Chondrite and primitive mantle values are from McDonough and Sun (1995).

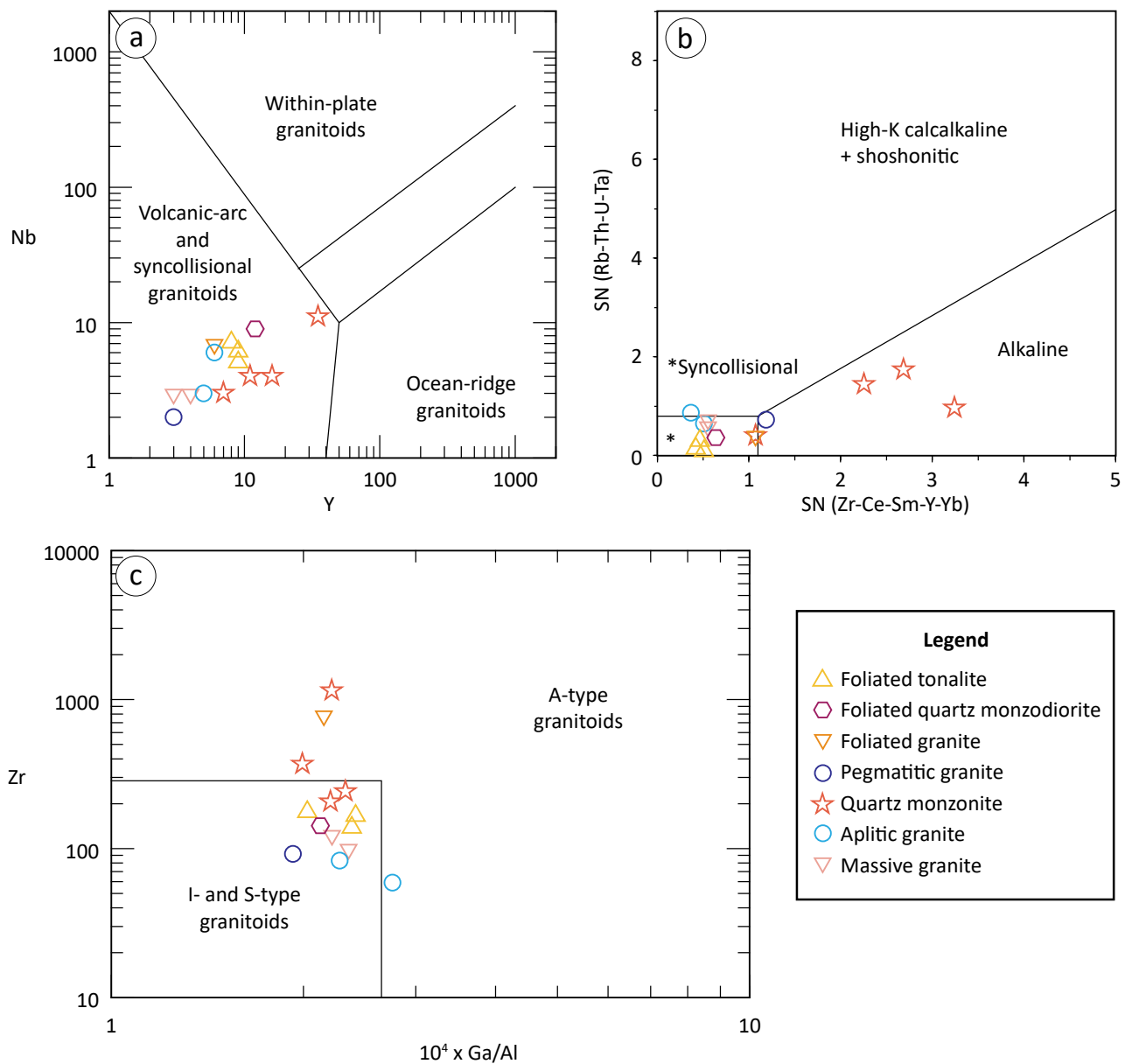


Figure 20: Discrimination diagrams showing the compositions of Huzyk Creek granitoids: **a)** Nb-Y diagram of Pearce et al. (1984); **b)** sliding normalization (SN) diagram of Liégeois et al. (1998); **c)** Zr-Ga/Al plot of Whalen et al. (1987).

are typically enriched in Ba and Sr (>1500 and >1000 ppm, respectively), contain significant CaO (2.16–12.06 wt. %), have intermediate Mg# values (0.20–0.65), and are depleted in Nb (1–40 ppm) and HREE ($[La/Lu]_N = 20–128$) with weak Eu anomalies ($Eu/Eu^* = 0.68–0.93$; Figure 24; Couëslan, 2005; Martins, 2012; Martins et al., 2012b; Martins, unpublished data, 2013). Published and preliminary ages for these intrusions range from ca. 1.83 to 1.79 Ga (Salnikova et al., 2019; Böhm, unpublished data, 2001; Martins, unpublished data, 2022), and overlap with the crystallization age of ca. 1801 Ma determined for the Huzyk Creek quartz monzonite. Therefore, the Huzyk Creek quartz monzonite likely shares affinity with the high-K calcalkaline to shoshonitic intrusions of the Trans-Hudson orogen.

Although carbonatite is known to be associated with two of the Trans-Hudson orogen shoshonitic complexes (Eden and Brez-

den lakes; Couëslan, 2005; Chakhmouradian et al., 2008; Hnatiuk et al., 2022), no carbonatite was identified in the drillcore from Huzyk Creek. However, biotite-carbonate microveinlets are ubiquitous in the quartz monzonite, and it is possible that they could be related to carbonatite magmatism. Isotopic and mineral geochemical studies of the carbonate veinlets may be warranted to investigate the potential for carbonatitic input.

Possible metasomatic phases

Examples of sulphide- and titanite-rich calcsilicate and bleached tonalite were identified as possible metasomatic phases during core logging based on textural and crosscutting relationships and enrichment of accessory phases. The bleached tonalite is a small zone of massive rock that appears to overprint the foliated tonalite. The groundmass of felted plagioclase and

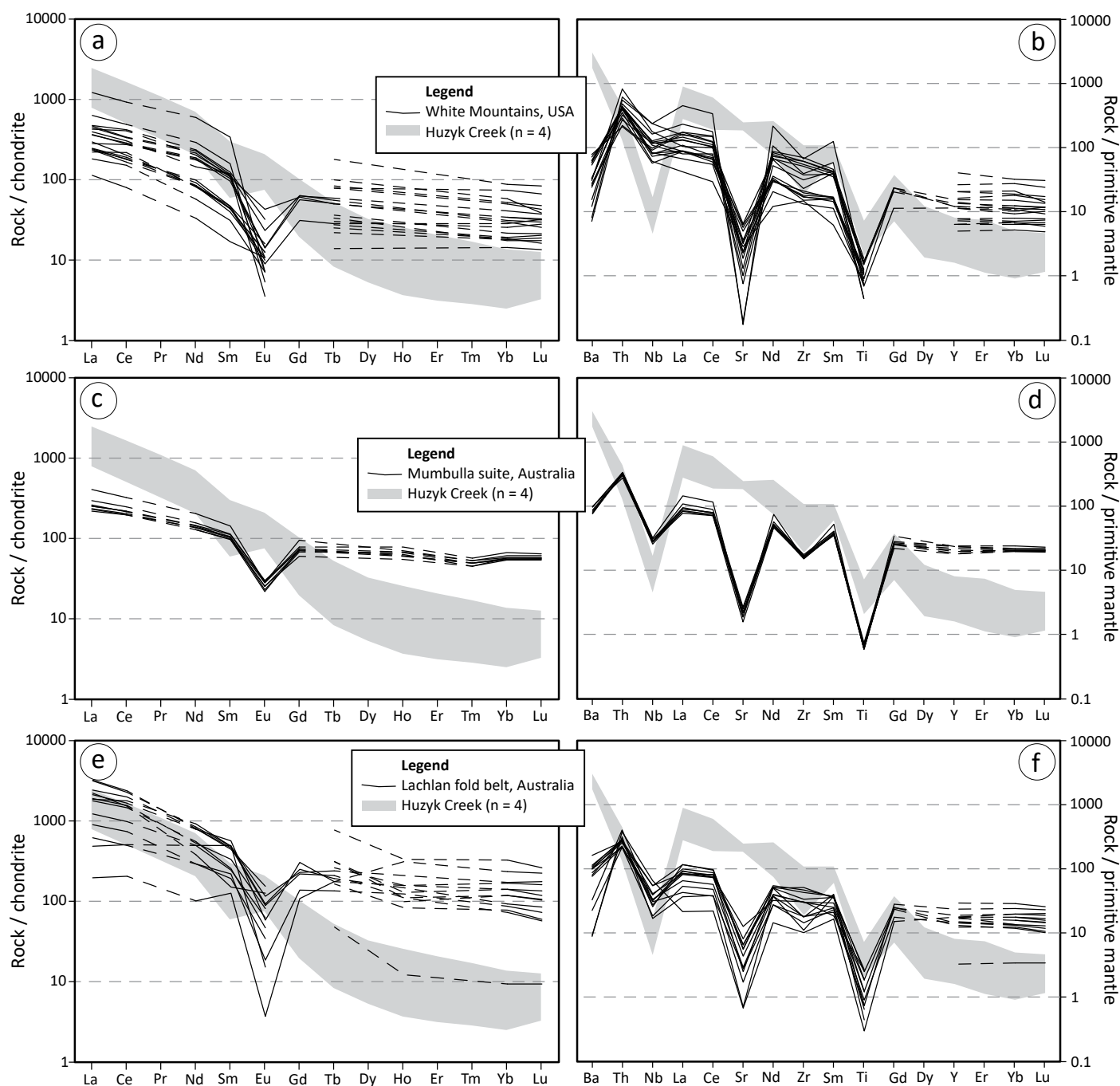


Figure 21: Chondrite-normalized REE profiles (left column) and primitive mantle-normalized multi-element profiles (right column) of representative A-type granite suites compared to the Huzyk Creek quartz monzonite. Dashed lines connect points that are separated by no data. Source data: chondrite and primitive mantle, McDonough and Sun (1995); Lachlan fold belt, King et al. (1997); Mumbulla suite, Collins et al. (1982); White Mountains, Eby (1990).

relative abundance of carbonate and allanite are suggestive of a metasomatic origin. The absence of foliation suggests the relative timing to be correlative with the younger suite of intrusions. The REE and multi-element profiles of the bleached tonalite are significantly different from those of the unaltered tonalite (Figure 25a, b). Only the most immobile elements (Nb, Zr, Ti and HREE) appear similar. All other elements are enriched in the bleached tonalite relative to the unaltered tonalite, as is S. The profiles of the bleached tonalite are very similar to those of the quartz monzonite, suggesting the metasomatizing fluid could have been related to the monzonite magmatism.

Trace-element geochemistry suggests two distinct populations of the calcsilicate, one that is enriched and one that is depleted. The enriched calcsilicate comprises the discordant calcsilicate and the sulphide-rich calcsilicate. Both types of enriched calcsilicate are non-foliated and appear to be vein-like structures overprinting the mafic gneiss suite. The REE and multi-element profiles of the mafic gneiss suite are characterized by a relatively smooth, shallow negative slope, and are distinctly different from those of the enriched calcsilicate (Figure 25c, d). The geochemical profiles of the enriched calcsilicate are more similar to the bleached tonalite and quartz monzonite (Figure 25a, b). The vein-

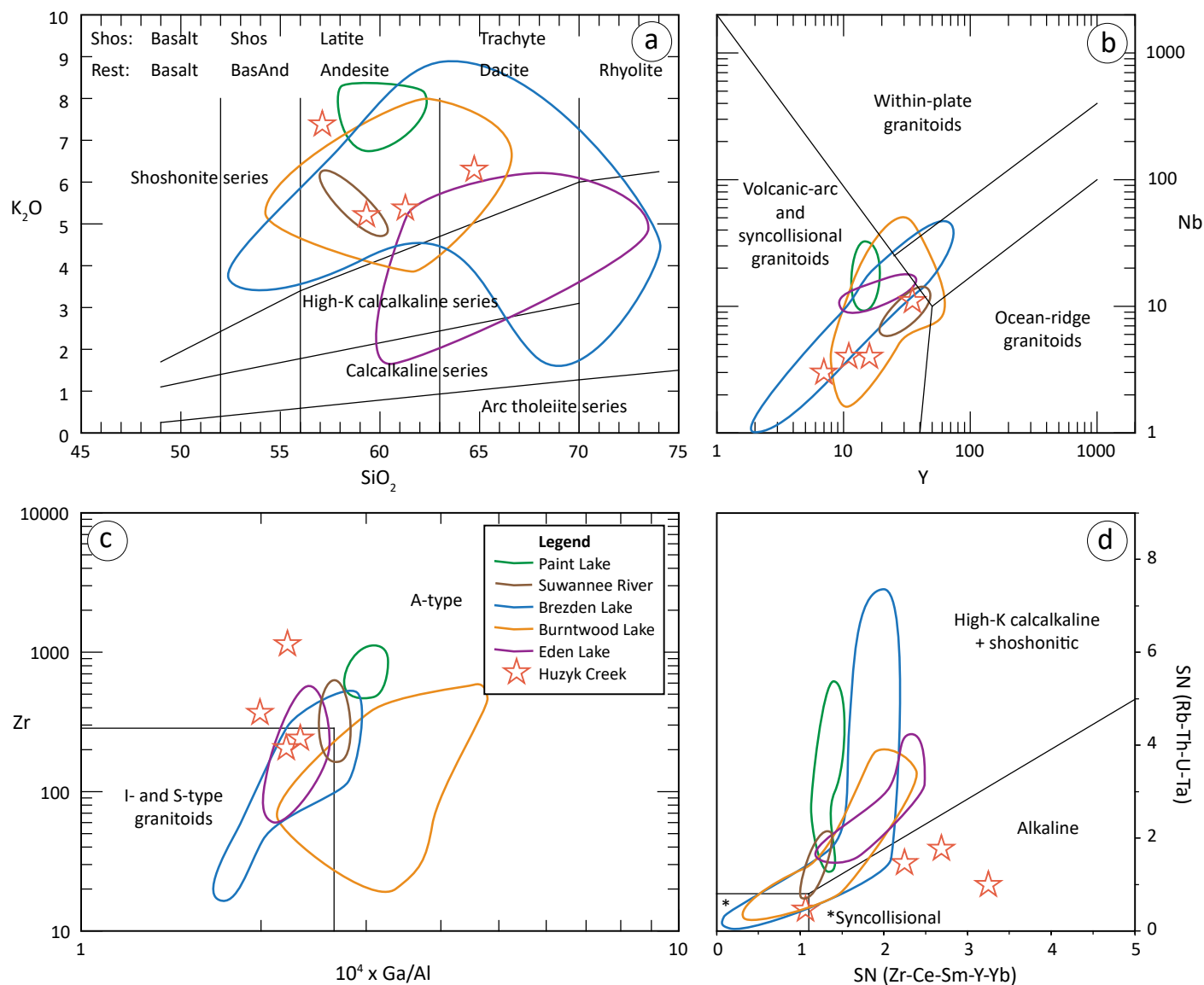


Figure 22: Discrimination diagrams showing the compositions of high-K to shoshonitic suites from the Trans-Hudson orogen, the Paint Lake syenite from the Thompson nickel belt, and the Huzyk Creek quartz monzonite: **a)** K_2O - SiO_2 diagram of Peccerillo and Taylor (1976); **b)** Nb-Y diagram of Pearce et al. (1984); **c)** Zr-Ga/Al plot of Whalen et al. (1987); **d)** sliding normalization diagram of Liégeois et al. (1998). Source data: Brezden Lake, Martins et al. (2012b); Burntwood Lake, Martins (2012); Eden Lake, Couëslan (2005); Paint Lake, Couëslan (2016); Suwannee River, Martins (unpublished data, 2013). Abbreviations: BasAnd, basaltic andesite; Shos, shoshonite/shoshonite series; SN, sliding normalization.

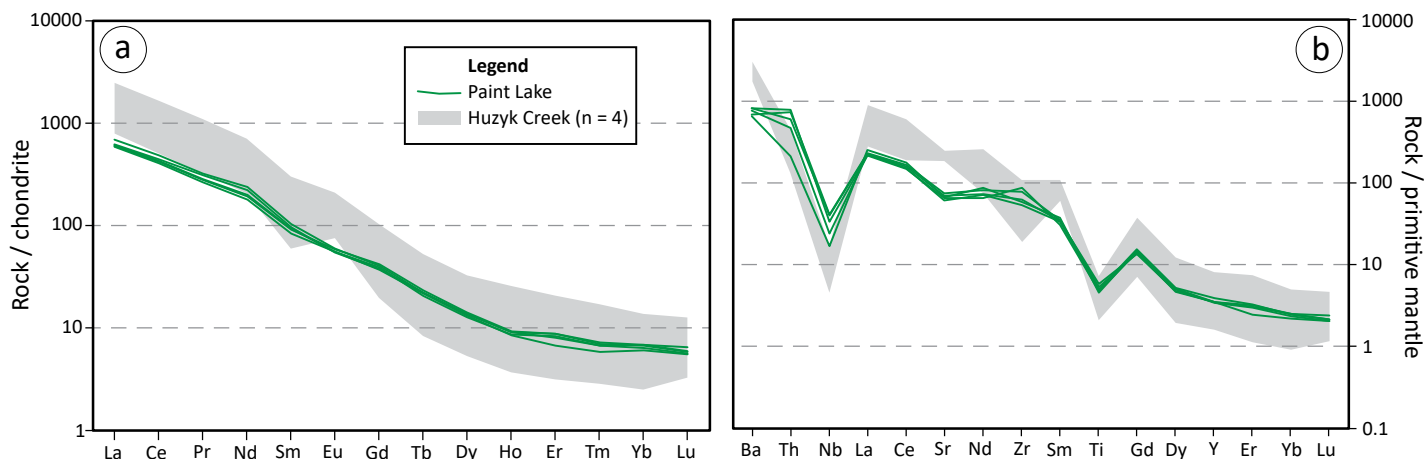


Figure 23: Chondrite-normalized REE profiles **(a)** and primitive mantle-normalized multi-element profiles **(b)** of the Paint Lake syenite compared to the Huzyk Creek quartz monzonite. Chondrite and primitive mantle values are from McDonough and Sun (1995).

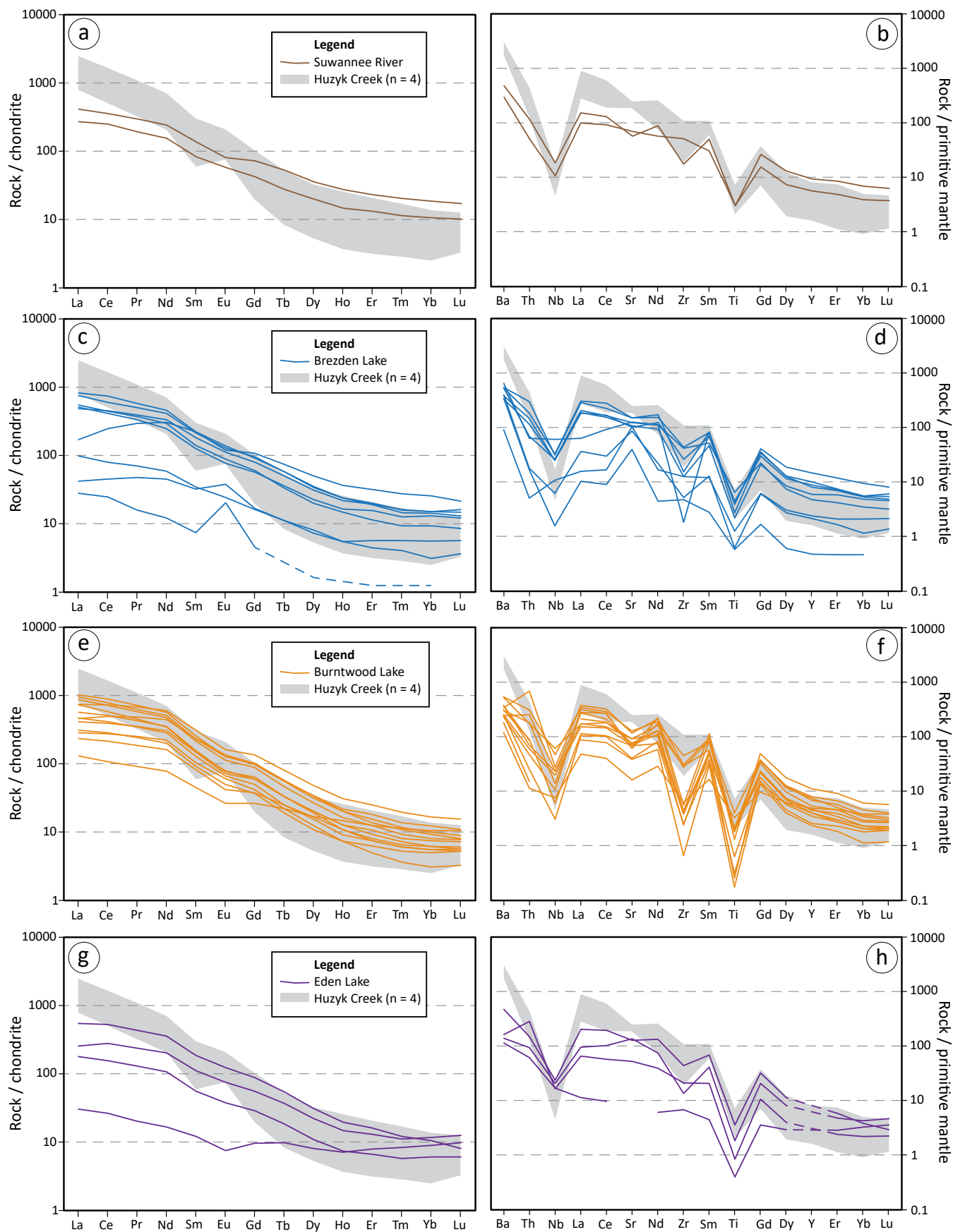


Figure 24: Chondrite-normalized REE profiles (left column) and primitive mantle-normalized multi-element profiles (right column) of high-K to shoshonitic suites from the Trans-Hudson orogen compared to the Huzyk Creek quartz monzonite. Source data: chondrite and primitive mantle, McDonough and Sun (1995); Brezden Lake, Martins et al. (2012); Burntwood Lake, Martins (2012); Eden Lake, Couëslan (2005); Suwannee River, Martins (unpublished data, 2013).

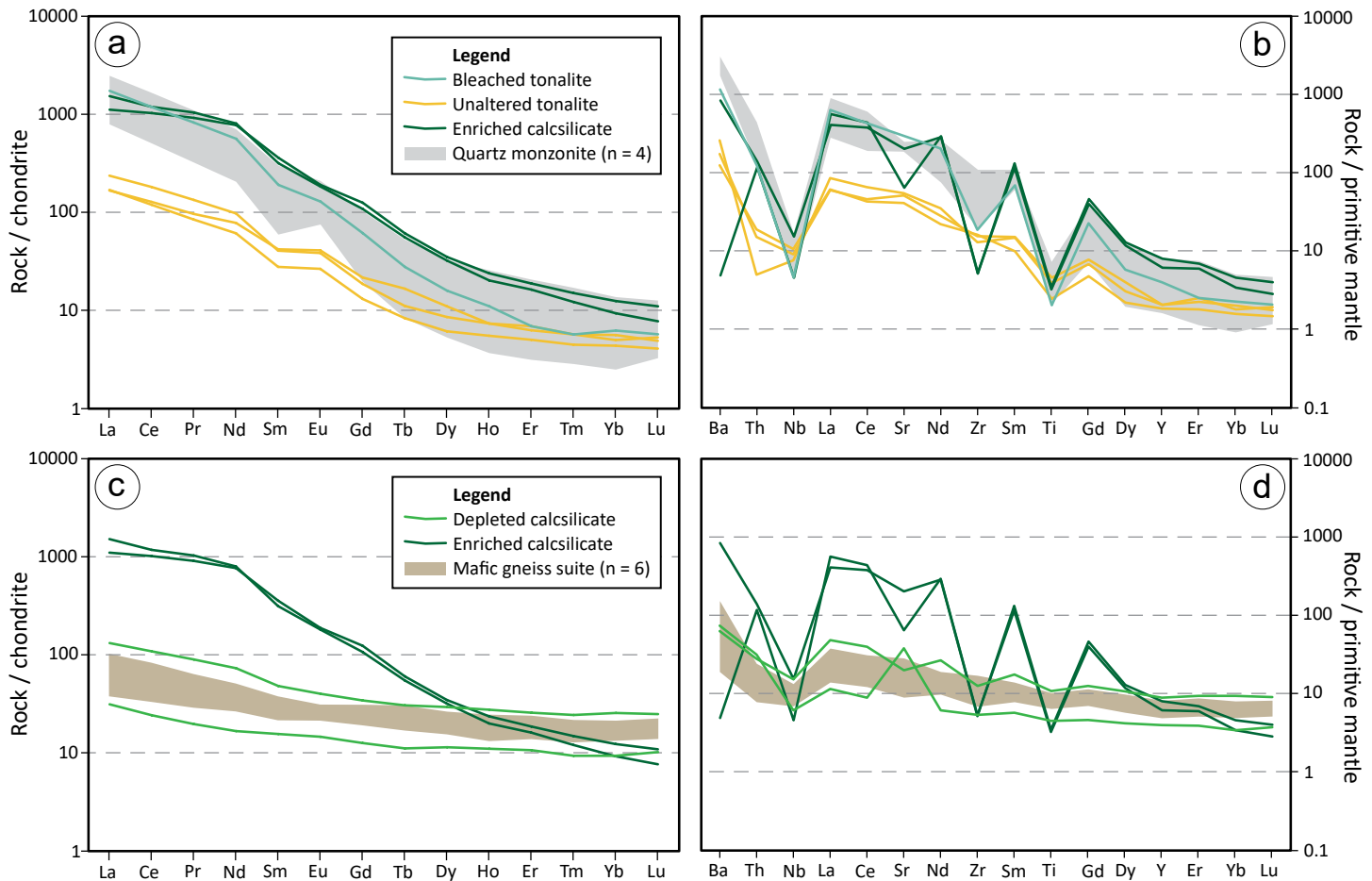


Figure 25: Chondrite-normalized REE profiles (**a**) and primitive mantle-normalized multi-element profiles (**b**) of the bleached tonalite and enriched calcsilicate compared to the unaltered tonalite and quartz monzonite; chondrite-normalized REE profiles (**c**) and primitive mantle-normalized multi-element profiles (**d**) of the depleted calcsilicate compared to the enriched calcsilicate and mafic gneiss suite. Source data: Chondrite and primitive mantle, McDonough and Sun (1995); mafic gneiss suite, Couëslan (2020c).

like character and lack of foliation suggest relatively late timing, and combined with the similarity in geochemistry, this could suggest an affinity to the quartz monzonite.

Conversely the profiles of the relatively depleted calcsilicate are most similar to the mafic gneiss suite (Figure 25c, d; Couëslan, 2020a). The depleted calcsilicate includes the semiconcordant calcsilicate and the foliated and titanite-rich calcsilicate. The foliated calcsilicate appears to be a xenolith entrained within the quartz monzonite. In addition, it has a well defined fabric that suggests it predates the intrusion of the host quartz monzonite. Although titanite does appear to be relatively abundant in this rock, the foliated calcsilicate does not appear to be related to the quartz monzonite as a metasomatic phase. The semiconcordant calcsilicate has a zoned vein-like structure with a diffuse selvage and massive core enriched in titanite and apatite. This suggests the semiconcordant calcsilicate is a relatively late feature, which is mineralogically distinct from rocks of the mafic gneiss suite. The diffuse nature of the selvage and the unusual abundance of apatite and titanite are suggestive of a metasomatic origin. However, the trace-element geochemistry does not suggest an affinity to the quartz monzonite.

Economic considerations

The Huzyk Creek quartz monzonite likely shares affinity with high-K calcalkaline to shoshonitic intrusive complexes in the Trans-Hudson orogen of Manitoba. Several of these complexes have been explored for U, Th, REE and P (McRitchie, 1987, 1988; Mumin, 2010; Assessment File 64C1124, Manitoba Economic Development, Investment and Trade, Winnipeg). Both REE and U are considered critical materials/minerals for Canada's economic security (Natural Resources Canada, 2021). The shoshonitic igneous complex at Eden Lake is associated with post-orogenic carbonatite magmatism and REE mineralization (Chakhmouradian et al., 2008; Martins, 2016) and carbonatite was recently discovered at the Brezden Lake complex (Hnatuk et al., 2022). Post-orogenic carbonatites are a major source for the global supply of REE and are frequently found in association with broadly shoshonitic rocks (e.g., Mountain Pass, California and Maoniuping, China; Hou et al., 2006, 2009; Castor, 2008; Watts et al., 2022). Although no carbonatite was identified in drillcore at Huzyk Creek, carbonate microveinlets are ubiquitous in the quartz monzonite. It is possible that these microveinlets are related to carbonatite magmatism. Isotopic and mineral geochemical studies

of the carbonate veinlets and possible metasomatic rocks may be warranted to investigate the potential for carbonatitic input.

Zircon is abundant in the Huzyk Creek quartz monzonite, with one sample containing 1143 ppm Zr. It is possible that cumulate layers or hydrothermal veins associated with the monzonite could be further enriched in Zr; however, the rocks identified as metasomatic are depleted in Zr relative to the monzonite, suggesting Zr was relatively immobile in the hydrothermal fluid(s). Although Canada does not consider Zr to be a critical material, both the United States and Australia have included Zr in their critical mineral lists (Schulz et al., 2017; Australian Trade and Investment Commission, 2020). Zirconium is used in the ceramics and nuclear energy industries, and for refractory and foundry applications (Sangine, 2017).

A genetic and/or spatial association exists between high-K calcalkaline and shoshonitic rocks, and some mesothermal and epithermal gold deposits, as well as Cu-Au porphyry and skarn systems (Müller and Groves, 1993, 2016; Robert, 2001; Sillitoe, 2002; Kelley et al., 2020). Disseminated sulphide is present in the quartz monzonite and there appears to be enrichment of sulphide in the metasomatic phases. The sulphide-rich calcsilicate also contains 1930 ppm Cu, 23 ppm Mo and 34 ppm As (Table 1; Couëslan, 2020c). Gold was not included in the analytical package. Although shoshonitic magmatism can be associated with base and precious metal deposits, these typically form at relatively shallow crustal depths. The coarse grain size and lack of brittle structures associated with the quartz monzonite and metasomatic phases at Huzyk Creek suggest that emplacement likely occurred at too great a depth to generate these deposit-types.

Acknowledgments

The author thanks E. Anderson for logistical support, and T. Martins for assistance and scientific discussion in the field. T. Martins and C. Böhm reviewed previous drafts of this Open File. Gogal Air Services provided access to the drillcore and their core logging facilities. Thanks to M. Simpson of Vanadian Energy Corp. for allowing access to, and sampling of, the drillcore.

References

- Ansdell, K.M., Lucas, S.B., Connors, K. and Stern, R.A. 1995: Kiseynew metasedimentary gneiss belt, Trans-Hudson orogen (Canada): back-arc origin and collisional inversion; *Geology*, v. 23, no. 11, p. 1039–1043.
- Australian Trade and Investment Commission 2020: Australian Critical Minerals Prospectus 2020; Commonwealth of Australia, 169 p.
- Bailes, A.H. 2015: Geological setting of the Watts River base metal massive sulphide deposit; HudBay Minerals Inc., unpublished internal geological report, 70 p.
- Beaumont-Smith, C. 2018: Geology report on the Huzyk Creek property, Ponton Manitoba region; NI 43-101 report prepared for Vanadian Energy Corp., 51 p., URL <https://www.sedar.com/search/search_form_pc_en.htm> [November 2022].
- Bonin, B. 2007: A-type granites and related rocks: evolution of a concept, problems, and prospects; *Lithos*, v. 97, p. 1–29.
- Castor, S.B. 2008: The Mountain Pass rare-earth carbonatite and associated ultrapotassic rocks, California; *The Canadian Mineralogist*, v. 46, p. 779–806.
- Chakhmouradian, A.R., Mumin, A.H., Demény, A. and Elliott, B. 2008: Postorogenic carbonatites at Eden Lake, Trans-Hudson Orogen (northern Manitoba, Canada): geological setting, mineralogy and geochemistry; *Lithos*, v. 103, p. 503–526.
- Collins, W.J., Beams, S.D., White, A.J.R. and Chappell, B.W. 1982: Nature and origin of A-type granites with particular reference to south-eastern Australia; *Contributions to Mineralogy and Petrology*, v. 80, p. 189–200.
- Corrigan, D., Pehrsson, S., Wodicka, N. and de Kemp, E. 2009: The Palaeoproterozoic Trans-Hudson Orogen: a prototype of modern accretionary processes; in *Ancient Orogens and Modern Analogues*, J.B. Murphy, J.D. Keppie and A.J. Hynes (ed.), Geological Society of London, Special Publications, v. 327, p. 457–479.
- Couëslan, C.G. 2005: Geochemistry and petrology of the Eden Lake carbonatite and associated silicate rocks; M.Sc. thesis, University of Western Ontario, London, Ontario, 201 p.
- Couëslan, C.G. 2016: Geology of the Paint and Phillips lakes area, Thompson nickel belt, central Manitoba (parts of NTS 63O1, 8, 9, 63P5, 12); Manitoba Growth, Enterprise and Trade, Manitoba Geological Survey, Geoscientific Report GR2016-1, 44 p., 1 map at 1:50 000 scale, URL <<https://manitoba.ca/iem/info/libmin/GR2016-1.zip>> [November 2022].
- Couëslan, C.G. 2019: Evaluation of graphite- and vanadium-bearing drillcore from the Huzyk Creek property, sub-Phanerozoic Kiseynew domain, central Manitoba (NTS 63J6); in *Report of Activities 2019*, Manitoba Agriculture and Resource Development, Manitoba Geological Survey, p. 60–71, URL <<https://manitoba.ca/iem/geo/field/roa19pdfs/GS2019-6.pdf>> [November 2022].
- Couëslan, C.G. 2020a: Geology and interpretation of graphite- and vanadium-enriched drillcore from the Huzyk Creek property, sub-Phanerozoic Kiseynew domain, central Manitoba (NTS 63J6); Manitoba Agriculture and Resource Development, Manitoba Geological Survey, Geoscientific Paper GP2020-1, 29 p., URL <<https://manitoba.ca/iem/info/libmin/GP2020-1.zip>> [November 2022].
- Couëslan, C.G. 2020b: Investigation of zirconium- and light rare-earth element-enriched rocks in drillcore from the Huzyk Creek property, sub-Phanerozoic Kiseynew domain, central Manitoba (NTS 63J6); in *Report of Activities 2020*, Manitoba Agriculture and Resource Development, Manitoba Geological Survey, p. 13–20.
- Couëslan, C.G. 2020c: Lithogeochemistry of drillcore from the Huzyk Creek property, central Manitoba (NTS 63J6); Manitoba Agriculture and Resource Development, Manitoba Geological Survey, Data Repository Item DRI2020028, Microsoft® Excel® file, URL <<https://manitoba.ca/iem/info/libmin/DRI2020028.xlsx>> [November 2022].
- Couëslan, C.G. 2022: Affinity and petrogenesis of the Huzyk Creek metal-enriched graphite deposit: a metamorphosed metalliferous black shale in the Trans-Hudson orogen of Manitoba, Canada; *The Canadian Mineralogist*, v. 60, p. 853–880.
- Eby, G.N. 1990: The A-type granitoids: a review of their occurrence and chemical characteristics and speculations on their petrogenesis; *Lithos*, v. 26, p. 115–134.
- Gerstenberger, H. and Haase, G. 1997: A highly effective emitter substance for mass spectrometric Pb isotope ratio determinations; *Chemical Geology*, v. 136, p. 309–312.
- Goldstein, S.L., O’Nions, R.K. and Hamilton, P.J. 1984: A Sm-Nd isotopic study of atmospheric dusts and particulates from major river systems; *Earth and Planetary Science Letters*, v. 70, p. 221–236.

- Hnatiuk, T., Couëslan, C.G., Chakhmouradian, A.R. and Martins, T. 2022: Preliminary results from targeted sampling of the Brezden Lake intrusive complex, west-central Manitoba (parts of NTS 64C4); *in* Report of Activities 2022, Manitoba Natural Resources and Northern Development, Manitoba Geological Survey, p. 42–48, URL <<https://manitoba.ca/iem/geo/field/roa22pdfs/GS2022-6.pdf>> [November 2022].
- Hou, Z., Tian, S., Yuan, Z., Xie, Y., Yin, S., Yi, L., Fei, H. and Yang, Z. 2006: The Himalayan collision zone carbonatites in western Sichuan, SW China: petrogenesis, mantle source and tectonic implication; *Earth and Planetary Science Letters*, v. 244, p. 234–250.
- Hou, Z., Tian, S., Xie, Y., Yang, Z., Yuan, Z., Yin, S., Yi, L., Fei, H., Zou, T., Bai, G. and Li, X. 2009: The Himalayan Mianing–Dechang REE belt associated with carbonatite–alkaline complexes, eastern Indo-Asian collision zone, SW China; *Ore Geology Reviews*, v. 36, p. 65–89.
- Kelley, K.D., Spry, P.G., McLemore, V.T., Fey, D.L. and Anderson, E.D. 2020: Alkaline-type epithermal gold deposit models; U.S. Geological Survey, Scientific Investigations Report 2010-5070-R, 74 p.
- King, P.L., White, A.J.R., Chappell, B.W. and Allen, C.M. 1997: Characterization and origin of aluminous A-type granites from the Lachlan Fold belt, southeastern Australia; *Journal of Petrology*, v. 38, p. 371–391.
- Krogh, T.E. 1973: A low-contamination method for hydrothermal decomposition of zircon and extraction of U and Pb for isotopic age determinations; *Geochimica et Cosmochimica Acta*, v. 37, p. 485–494.
- Leclair, A.D., Lucas, S.B., Broome, H.J., Viljoen, D.W. and Weber, W. 1997: Regional mapping of Precambrian basement beneath Phanerozoic cover in southeastern Trans-Hudson Orogen, Manitoba and Saskatchewan; *Canadian Journal of Earth Sciences*, v. 34, p. 618–634.
- Le Maitre, R.W. 2002: *Igneous rocks: a classification and glossary of terms*; Cambridge University Press, Cambridge, United Kingdom, 236 p.
- Lewry, J.F., Thomas, D.J., Macdonald, R. and Chiarenzelli, J. 1990: Structural relations in accreted terranes of the Trans-Hudson Orogen, Saskatchewan: telescoping in a collisional regime?; *in* The Early Proterozoic Trans-Hudson Orogen of North America, J.F. Lewry and M.R. Stauffer (ed.), Geological Association of Canada, Special Paper 37, p. 75–94.
- Liégeois, J.-P., Navez, J., Hertogen, J. and Black, R. 1998: Contrasting origin of post-collisional high-K calc-alkaline and shoshonitic versus alkaline and peralkaline granitoids. The use of sliding normalization; *Lithos*, v. 45, p. 1–28.
- Ludwig, K.R. 2012: User's Manual for Isoplot 3.75: a geochronological toolkit for Microsoft® Excel®; Berkeley Geochronological Center, Special Publication 5, 75 p.
- Maniar, P.D. and Piccoli, P.M. 1989: Tectonic discrimination of granitoids; *Geological Society of America Bulletin*, v. 101, p. 635–643.
- Manitoba Geological Survey 2021: Compilation of Sm-Nd isotope results from the Manitoba Geological Survey 2020/2021 season; Manitoba Agriculture and Resource Development, Manitoba Geological Survey, Data Repository Item DRI2021005, Microsoft® Excel® file, URL <<https://manitoba.ca/iem/info/libmin/DRI2021005.xlsx>> [November 2022].
- Manitoba Geological Survey 2022: Bedrock geology of Manitoba; Manitoba Natural Resources and Northern Development, Manitoba Geological Survey, Open File OF2022-2, scale 1:1 000 000, URL <<https://manitoba.ca/iem/info/libmin/OF2022-2.zip>> [November 2022].
- Martins, T. 2012: Whole-rock geochemistry of the Burntwood Lake alkali-feldspar syenite, west-central Manitoba (part of NTS 63N8); Manitoba Innovation, Energy and Mines, Manitoba Geological Survey, Data Repository Item DRI2012001, Microsoft® Excel® file, URL <<https://manitoba.ca/iem/info/libmin/DRI2012001.xls>> [November 2022].
- Martins, T. 2016: Rare metals in Manitoba: Eden Lake carbonatite complex; Manitoba Growth, Enterprise and Trade, Manitoba Geological Survey, URL <<http://manitoba.ca/iem/geo/raremetals/pdfs/edenlake.pdf>> [March 2020].
- Martins, T. and Couëslan, C.G. 2022: Critical minerals scoping study of the Suwannee River syenite intrusion, west-central Manitoba (part of NTS 64B4); *in* Report of Activities 2022, Manitoba Natural Resources and Northern Development, Manitoba Geological Survey, p. 36–41, URL <<https://manitoba.ca/iem/geo/field/roa22pdfs/GS2022-5.pdf>> [November 2022].
- Martins, T., Couëslan, C.G. and Böhm, C.O. 2011: The Burntwood Lake alkali-feldspar syenite revisited, west-central Manitoba (part of NTS 63N8); *in* Report of Activities 2011, Manitoba Innovation, Energy and Mines, Manitoba Geological Survey, p. 79–85, URL <<https://manitoba.ca/iem/geo/field/roa11pdfs/GS-8.pdf>> [November 2022].
- Martins, T., Couëslan, C.G. and Böhm, C.O. 2012a: Rare metals scoping study of the Brezden Lake intrusive complex, western Manitoba (part of NTS 64C4); *in* Report of Activities 2012, Manitoba Innovation, Energy and Mines, Manitoba Geological Survey, p. 115–123, URL <<https://manitoba.ca/iem/geo/field/roa12pdfs/GS-10.pdf>> [November 2022].
- Martins, T., Couëslan, C.G. and Böhm, C.O. 2012b: Rare metals scoping study of the Brezden Lake intrusive complex, western Manitoba (part of NTS 64C4); Manitoba Innovation, Energy and Mines, Manitoba Geological Survey, Data Repository Item DRI2012006, Microsoft® Excel® file, URL <<https://manitoba.ca/iem/info/libmin/DRI2012006.xls>> [November 2022].
- Mattinson, J.M. 2005: Zircon U-Pb chemical abrasion ("CA-TIMS") method: combined annealing and multi-step partial dissolution analysis for improved precision and accuracy of zircon ages; *Chemical Geology*, v. 220, p. 47–66.
- Maxeiner, R.O., Ashton, K.E., Bosman, S.A., Card, C.D., Kohlruss, D., Marsh, A., Morelli, R. and Slimmon, W.L. 2021: Notes to accompany the new 2021 edition of the 1:1 000 000-scale geological map of Saskatchewan; Saskatchewan Geological Survey, Saskatchewan Ministry of Energy and Resources, Miscellaneous Report 2021-2, 20 p.
- McDonough, W.F. and Sun, S.-s. 1995: The composition of the Earth; *Chemical Geology*, v. 120, p. 223–253.
- McRitchie, W.D. 1987: Burntwood Lake syenite; *in* Report of Field Activities 1987, Manitoba Energy and Mines, Minerals Division, p. 65–69, URL <<https://manitoba.ca/iem/geo/field/roa87.pdf>> [November 2022].
- McRitchie, W.D. 1988: Alkaline intrusions of the Churchill Province, Eden Lake (64C/9) and Brezden Lake (64C/4); *in* Report of Field Activities 1988, Manitoba Energy and Mines, Minerals Division, p. 5–11, URL <<https://manitoba.ca/iem/geo/field/rfa88.zip>> [November 2022].
- Müller, D. and Groves, D.I. 1993: Direct and indirect associations between potassic igneous rocks, shoshonites and gold-copper deposits; *Ore Geology Reviews*, v. 8, p. 383–406.
- Müller, D. and Groves, D.I. 2016: *Potassic igneous rocks and associated gold-copper mineralization* (4th edition); Springer Cham, Switzerland, 311 p.
- Mumin, H. 2010: The Eden Lake rare metal (REE, Y, U, Th, phosphate) carbonatite complex, Manitoba: updated report; Medallion Resources Ltd., NI 43-101 report, 110 p., 6 appendices.
- Murphy, L.A. and Zwanzig, H.V. 2021: Geology of the Wuskwatim–Granville lakes corridor, Kiseeynew domain, Manitoba (parts of NTS 63O, P, 64A–C); Manitoba Agriculture and Resource Development, Manitoba Geological Survey, Geoscientific Report GR2021-2, 94 p.
- Natural Resources Canada 2021: Critical minerals; Natural Resources Canada, URL <<https://www.nrcan.gc.ca/our-natural-resources/minerals-mining/critical-minerals/23414>> [May 2021].

- Pearce, J.A., Harris, N.B.W. and Tindle, A.G. 1984: Trace element discrimination diagrams for the tectonic interpretation of granitic rocks; *Journal of Petrology*, v. 25, p. 956–983.
- Peccerillo, A. and Taylor, S.R. 1976: Geochemistry of eocene calc-alkaline volcanic rocks from the Kastamonu area, northern Turkey; *Contributions to Mineralogy and Petrology*, v. 58, p. 63–81.
- Rayner, N. and Percival, J.A. 2007: Uranium-lead geochronology of basement units in the Wuskwatim–Tullibee lakes area, northeastern Kiseynew Domain, Manitoba (NTS 63O); *in* Report of Activities 2007, Manitoba Science, Technology, Energy and Mines, Manitoba Geological Survey, p. 82–90, URL <<https://manitoba.ca/iem/geo/field/roa07pdfs/GS-8.pdf>> [November 2022].
- Reid, K.D. 2018: Sub-Phanerozoic basement geology from drillcore observations in the Watts, Mitishtio and Hargrave rivers area, eastern Flin Flon belt, west-central Manitoba (parts of NTS 63J5, 6, 11, 12, 13, 14); *in* Report of Activities 2018, Manitoba Growth, Enterprise and Trade, Manitoba Geological Survey, p. 37–47, URL <<https://manitoba.ca/iem/geo/field/roa18pdfs/GS2018-4.pdf>> [November 2022].
- Robert, F. 2001: Syenite-associated disseminated gold deposits in the Abitibi greenstone belt, Canada; *Mineralium Deposita*, v. 36, p. 503–516.
- Salnikova, E.B., Chakhmouradian, A.R., Stifeeva, M.V., Reguir, E.P., Kotov, A.B., Gritsenko, Y.D. and Nikiforov, A.V. 2019: Calcic garnets as a geochronological and petrogenetic tool applicable to a wide variety of rocks; *Lithos*, v. 338–339, p. 141–154.
- Sangine, E. 2017: Zirconium and hafnium; *in* Critical Mineral Resources of the United States—Economic and Environmental Geology and Prospects for Future Supply, K.J. Schulz, J.H. DeYoung, Jr., R.R. Seal, II and D.C. Bradley (ed.), U.S. Geological Survey, Professional Paper 1802, p. J1–J24.
- Schmidberger, S.S., Simonetti, A., Heaman, L.M., Creaser, R.A. and Whitford, S. 2007: Lu–Hf, in-situ Sr and Pb isotope and trace element systematics for mantle eclogites from the Diavik diamond mine: evidence for Paleoproterozoic subduction beneath the Slave craton, Canada; *Earth and Planetary Science Letters*, v. 254, p. 55–68.
- Schulz, K.J., DeYoung, J.H., Jr., Seal, R.R., II and Bradley, D.C. (ed.) 2017: Critical mineral resources of the United States—economic and environmental geology and prospects for future supply; U.S. Geological Survey, Professional Paper 1802, 797 p.
- Sillitoe, R.H. 2002: Some metallogenic features of gold and copper deposits related to alkaline rocks and consequences for exploration; *Mineralium Deposita*, v. 37, p. 4–13.
- Simard, R.-L., McGregor, C.R., Rayner, N. and Creaser, R.A. 2010: New geological mapping, geochemical, Sm–Nd isotopic and U–Pb age data for the eastern sub-Phanerozoic Flin Flon belt, west-central Manitoba (parts of NTS 63J3–6, 11, 12, 14, 63K1–2, 7–10); *in* Report of Activities 2010, Manitoba Innovation, Energy and Mines, Manitoba Geological Survey, p. 69–87, URL <<https://manitoba.ca/iem/geo/field/roa10pdfs/GS-6.pdf>> [November 2022].
- Stacey, J.S. and Kramers, J.D. 1975: Approximation of terrestrial lead isotope evolution by a two-stage model; *Earth and Planetary Science Letters*, v. 26, p. 207–221.
- Stauffer, M.R. 1990: The Missi Formation: an Aphebian molasse deposit in the Reindeer Lake zone of the Trans-Hudson orogen, Canada; *in* The Early Proterozoic Trans-Hudson Orogen of North America, J.F. Lewry and M.R. Stauffer (ed.), Geological Association of Canada, Special Paper 37, p. 121–141.
- Unterschutz, J.L.E., Creaser, R.A., Erdmer, P., Thompson, R.I. and Daughtry, K.L. 2002: North American margin origin of Quesnel terrane strata in the southern Canadian Cordillera: inferences from geochemical and Nd isotopic characteristics of Triassic metasedimentary rocks; *Geological Society of America Bulletin*, v. 114, p. 462–475.
- Vanadian Energy Corporation 2019: Vanadian Energy intersects 0.22% V₂O₅ over 9.74 metres on the Huzyk Creek property; Vanadian Energy Corporation, press release, May 21, 2019, URL <<https://www.vanadianenergy.com/NR-2019-05-21-Drilling-results.pdf>> [June 2019].
- Watts, K.E., Haxel, G.B. and Miller, D.M. 2022: Temporal and petrogenetic links between Mesoproterozoic alkaline and carbonatite magmas at Mountains Pass, California; *Economic Geology*, v. 117, p. 1–23.
- Whalen, J.B., Currie, K.L. and Chappell, B.W. 1987: A-type granites: geochemical characteristics, discrimination and petrogenesis; *Contributions to Mineralogy and Petrology*, v. 95, p. 407–419.
- Zwanig, H.V. 1997: Comments on “Kiseynew metasedimentary gneiss belt, Trans-Hudson orogen (Canada): back-arc origin and collisional inversion” by Ansdell et al., 1995 (*Geology*, v. 23, p. 1039–1043); *Geology*, v. 25, p. 90–91.
- Zwanig, H.V. 1999: Structure and stratigraphy of the south flank of the Kiseynew Domain in the Trans-Hudson Orogen, Manitoba: implications for 1.845–1.77 Ga collision tectonics; *Canadian Journal of Earth Sciences*, v. 36, p. 1859–1880.
- Zwanig, H.V. and Bailes, A.H. 2010: Geology and geochemical evolution of the northern Flin Flon and southern Kiseynew domains, Kiseynew–File lakes area, Manitoba (parts of NTS 63K, N); Manitoba Innovation, Energy and Mines, Manitoba Geological Survey, Geoscientific Report GR2010-1, 135 p., URL <<https://manitoba.ca/iem/info/libmin/GR2010-1.zip>> [November 2022].